tumours of pure GGO, with no solid component and larger than 20 mm in size, would be candidates for limited surgical resection such as segmentectomy with nodal dissection. This information may also be useful for treating early lung cancers, with the advantages of maintained lung function and a reasonable prognosis.

The other significant predictor of pN0 disease was the presence of air bronchogram in the primary nodules. Air bronchogram is a radiographical finding, an air-filled bronchus surrounded by fluid-filled airspaces, and is mostly identified in areas with a slight, homogeneous increase in density on thin-section CT, such as GGO. However, with an increase in density and the solid component of primary nodules, it can be difficult to detect the underlying bronchovascular structure [15]. Disappearance of air bronchogram in the primary nodules shows that consolidation replaced GGO as a main component and its structure collapsed from a lepidic growth pattern [16–18].

One of the major limitations of this study is that few patients with resectable early lung cancer developed recurrence or other medical conditions in this short follow-up period, and we could not evaluate the correlation between the long-term prognosis and radiological findings, such as the maximum dimension of consolidation and the presence of air bronchogram.

In conclusion, this study showed that clinical stage IA lung cancer patients with consolidation had worse outcomes than those without consolidation. The maximum dimension of consolidation was an independent unfavourable prognostic factor, regardless of the maximum tumour dimension. The maximum dimension of consolidation was an upstaging factor for the T classification.

**Conflict of interest:** none declared.

## REFERENCES

[1] Aoki T, Tomoda Y, Watanabe H, Nakata H, Kasai T, Hashimoto H *et al.* Peripheral lung adenocarcinoma: correlation of thin-section CT findings with histologic prognostic factors and survival. Radiology 2001;220: 803–9.

[2] Takamochi K, Nagai K, Yoshida J, Suzuki K, Ohde Y, Nishimura M *et al.* Pathologic N0 status in pulmonary adenocarcinoma is predictable by combining serum carcinoembryonic antigen level and computed tomographic findings. J Thorac Cardiovasc Surg 2001;122:325–30.

[3] Suzuki K, Asamura H, Kusumoto M, Kondo H, Tsuchiya R. "Early" peripheral lung cancer: prognostic significance of ground glass opacity on thin-section computed tomographic scan. Ann Thorac Surg 2002;74: 1635–9.

[4] Suzuki K, Yokose T, Yoshida J, Nishimura M, Takahashi K, Nagai K *et al.* Prognostic significance of the size of central fibrosis in peripheral adenocarcinoma of the lung. Ann Thorac Surg 2000;69:893–7.

[5] Suzuki K, Koike T, Asakawa T, Kusumoto M, Asamura H, Nagai K *et al.* A prospective radiological study of thin-section computed tomography to predict pathological noninvasiveness in peripheral clinical IA lung cancer (Japan Clinical Oncology Group 0201). J Thorac Oncol 2011;6: 751–6.

[6] Ginsberg RJ, Rubinstein LV. Randomized trial of lobectomy versus limited resection for T1 N0 non-small cell lung cancer. Lung Cancer Study Group. Ann Thorac Surg 1995;60:615–22; discussion 622–613.

[7] Naruke T, Suemasu K, Ishikawa S. Lymph node mapping and curability at various levels of metastasis in resected lung cancer. J Thorac Cardiovasc Surg 1978;76:832–9.

[8] Kodama K, Higashiyama M, Yokouchi H, Takami K, Kuriyama K, Mano M *et al.* Prognostic value of ground-glass opacity found in small lung adenocarcinoma on high-resolution CT scanning. Lung Cancer 2001;33: 17–25.

[9] Maeshima AM, Tochigi N, Yoshida A, Asamura H, Tsuta K, Tsuda H. Histological scoring for small lung adenocarcinomas 2 cm or less in diameter: a reliable prognostic indicator. J Thorac Oncol 2010;5:333–9.

[10] Suzuki K, Kusumoto M, Watanabe S, Tsuchiya R, Asamura H. Radiologic classification of small adenocarcinoma of the lung: radiologic-pathologic correlation and its prognostic impact. Ann Thorac Surg 2006;81:413–9.

[11] Inoue M, Minami M, Sawabata N, Utsumi T, Kadota Y, Shigemura N *et al.* Clinical outcome of resected solid-type small-sized c-stage IA non-small cell lung cancer. Eur J Cardiothorac Surg 2010;37:1445–9.

[12] Ohtaki Y, Yoshida J, Ishii G, Aokage K, Hishida T, Nishimura M *et al.* Prognostic significance of a solid component in pulmonary adenocarcinoma. Ann Thorac Surg 2011;91:1051–7.

[13] Tsubota N, Ayabe K, Doi O, Mori T, Namikawa S, Taki T *et al.* Ongoing prospective study of segmentectomy for small lung tumors. Study Group of Extended Segmentectomy for Small Lung Tumor. Ann Thorac Surg 1998;66:1787–90.

[14] Okada M, Koike T, Higashiyama M, Yamato Y, Kodama K, Tsubota N. Radical sublobar resection for small-sized non-small cell lung cancer: a multicenter study. J Thorac Cardiovasc Surg 2006;132:769–75.

[15] Yoshino I, Ichinose Y, Nagashima A, Takeo S, Motohiro A, Yano T *et al.* Clinical characterization of node-negative lung adenocarcinoma: results of a prospective investigation. J Thorac Oncol 2006;1:825–31.

[16] Travis WD, Brambilla E, Noguchi M, Nicholson AG, Geisinger KR, Yatabe Y *et al.* International association for the study of lung cancer/American thoracic society/European respiratory society international multidisciplinary classification of lung adenocarcinoma. J Thorac Oncol 2011;6: 244–85.

[17] Warth A, Muley T, Meister M, Stenzinger A, Thomas M, Schirmacher P *et al.* The novel histologic international association for the study of Lung Cancer/American Thoracic Society/European Respiratory Society classification system of lung adenocarcinoma is a stage-independent predictor of survival. J Clin Oncol 2012;30:1438–46.

[18] Shim HS, Lee da H, Park EJ, Kim SH. Histopathologic characteristics of lung adenocarcinomas with epidermal growth factor receptor mutations in the International Association for the Study of Lung Cancer/American Thoracic Society/European Respiratory Society lung adenocarcinoma classification. Arch Pathol Lab Med 2011;135:1329–34.

European Journal of Cardio-Thoracic Surgery Advance Access published December 11, 2012

European Journal of Cardio-Thoracic Surgery (2012) 1-5
doi:10.1093/ejcts/ezs604

ORIGINAL ARTICLE

THORACIC

# The maximum standardized uptake value of fluorodeoxyglucose positron emission tomography of the primary tumour is a good predictor of pathological nodal involvement in clinical N0 non-small-cell lung cancer†

Yoshikazu Miyasaka, Kenji Suzuki*, Kazuya Takamochi, Takeshi Matsunaga and Shiaki Oh

Department of General Thoracic Surgery, Juntendo University School of Medicine, Tokyo, Japan

* Corresponding author. Department of General Thoracic Surgery, Juntendo University School of Medicine, 1-3, Hongo 3-chome, Bunkyo-ku, Tokyo 113-8431, Japan. Tel: +81-3-38133111; fax: +81-3-58000281; e-mail: kjsuzuki@juntendo.ac.jp (K. Suzuki).

Received 21 August 2012; received in revised form 8 October 2012; accepted 22 October 2012

## Abstract

**OBJECTIVES**: Fluorodeoxyglucose positron emission tomography (FDG-PET) plays an important role in the evaluation of resectable non-small-cell lung cancer (NSCLC). However, this modality cannot be used to detect histological nodal involvement, which can result in stage-migration for resectable lung cancer. In this study, we tried to evaluate the possibility of predicting histological nodal involvement in patients with NSCLC using the maximum standardized uptake value (SUVmax) of FDG-PET of the primary tumour instead of that of the lymph nodes.

**METHODS**: Between February 2008 and September 2011, 898 patients underwent lung cancer surgery at our institute. Among them, we retrospectively analysed 265 patients with clinical N0 NSCLC, who underwent preoperative FDG-PET. The relationships between clinicopathological features, including the findings of FDG-PET and pathological nodal involvement, were investigated. The factors investigated were age, gender, preoperative carcinoembryonic antigen titre, maximum tumour dimension, consolidation/tumour dimension ratio (C/T ratio), SUVmax in the primary tumour and smoking history.

**RESULTS**: Of the 265 clinical N0 NSCLC patients, 214 (80.8%) had pathological N0 status and 27 (10.2%) and 24 (9.0%) had pathological N1 and N2 disease. In a multivariate analysis, the C/T ratio ($P = 0.046$) and SUVmax of the primary tumour ($P = 0.016$) were significant predictors of pathological nodal involvement. With regard to pathological N1-2 disease, the sensitivity, specificity, accuracy and positive and negative predictive values of mediastinal node involvement in patients with NSCLC with an SUVmax for FDG-PET of 10 or more were 49.0, 83.2, 76.6, 41.0 and 87.3%, respectively. Of the 61 patients with NSCLC with an SUVmax for FDG-PET of 10 or more, 25 (41.0%) had pathological N1-2 disease, while only 26 (12.7%) of the remaining 204 patients with an SUVmax for FDG-PET of <10 had nodal disease ($P < 0.0001$).

**CONCLUSIONS**: Postoperative nodal status was significantly predicted by the SUVmax of FDG-PET of the primary tumour instead of the lymph nodes themselves. The patients with NSCLC in particular who show strong uptake values of SUVmax in the primary tumour could have occult nodal metastases, and may be indicated for a further preoperative modality for an accurate staging.

**Keywords:** Fluorodeoxyglucose positron emission tomography • Non-small-cell lung cancer • Pathological nodal involvement

## INTRODUCTION

Fluorodeoxyglucose positron emission tomography (FDG-PET) plays an important role in evaluating resectable non-small-cell lung cancer (NSCLC). Several authors have reported evidence that supports the clinical value of FDG-PET for lymph node staging in NSCLC [1-4]. However, this modality cannot be used to detect histological nodal involvement, which results in stage migration for resectable lung cancer. In fact, false PET results are not uncommon. In this study, we tried to evaluate the possibility of predicting histological nodal involvement in patients with NSCLC by using the maximum standardized uptake value (SUVmax) of FDG-PET of the primary tumour instead of that of the lymph nodes themselves.

†Presented at the 19th European Conference on General Thoracic Surgery, Marseille, France, 5-8 June 2011.

## MATERIALS AND METHODS

### Patient selection

Between February 2008 and September 2011, 898 patients underwent lung cancer surgery at our institute. Among them, we

retrospectively analysed 265 patients with clinical N0 (cN0) NSCLC who underwent preoperative computed tomography (CT) scan and FDG-PET, and who received lobectomy or segmentectomy with the systematic evaluation of both hilar and mediastinal lymph nodes. In all patients, the time interval between surgery to CT scan and FDG-PET was <1 month. The staging system for lung cancer was on the basis of the seventh TNM classification of the International Union against Cancer (UICC). Histological findings were determined according to the World Health Organization (WHO) classification. Nodal status was defined preoperatively on the basis of the findings of thoracic thin-section CT and PET scan. The criterion for cN0 was a short-axis of the nodes of <10 mm on the basis of CT and an SUV of <2.5 for nodes on FDG-PET. The cN0 patients did not undergo any type of preoperative invasive mediastinal staging, such as endobronchial ultrasound transbronchial nodal aspiration cytology (EBUS-TBNA) or mediastinoscopy.

In this study, we excluded patients with NSCLC who showed both ground-glass opacity (GGO) with a consolidation/tumour dimension (C/T) ratio of 50% or less, a maximum tumour dimension of 2 cm or less, and those with tumour that could be removed by limited resection. Such small-sized lung cancer on chest CT scan has been reported to show no invasive carcinoma and no lymph node involvement [5, 6]. This is why we enrolled such lesions in randomized controlled trials (Japan Clinical Oncology Group 0804 study) on limited resection for small-sized lung carcinoma. In the JCOG 0804 study, systematic lymph node dissection was not provided if there was no regional lymph nodes metastasis.

## Preoperative evaluation

The clinical records of each patient were reviewed to determine the following values: age, gender, histological findings, C/T ratio in the primary tumour on preoperative CT scan, preoperative carcinoembryonic antigen (CEA) titre, SUVmax in the primary tumour, clinical stage and smoking status. For the smoking status, we used categories of pack-years. All CT scans were reviewed. A contrast-enhanced CT scan was performed to evaluate the entire lung for preoperative staging. In addition, the main tumour was evaluated preoperatively by thin-section helical CT scan with 1–3 mm collimation to estimate the extent of GGO. Images were reconstructed with a field of view of 15–20 cm. The lung was photographed with a window level of− 500 to− 700 H and a window width of 1000–2000 H as a 'lung window,' and with a window level of 30–60 H and a window width of 350–600 H as a 'mediastinal window'. The consolidation component was defined as an area of increased opacification that completely obscured the underlying vascular markings. GGO was defined as an area of a slight, homogenous increase in density that did not obscure the underlying vascular markings. Minimally-invasive lung cancer was tentatively defined as a tumour in which the ratio of the maximum diameter of consolidation to the maximum tumour diameter (C/T ratio) was <0.5, which would indicate a tumour with a wide GGO area. Thus, we considered the C/T ratio (≥0.5, <0.5) in our investigation.

## Statistical analysis

Statistical analyses were performed using SPSS 10.0 software (SPSS, Inc., Chicago, IL, USA). For the comparisons of pathological nodal involvement and the clinical factors, categorical and continuous variables were analysed by the chi-square test and unpaired *t*-test, respectively. Statistical analysis was performed with uni- and multivariate analyses using logistic regression analysis. The factors investigated were age, gender, histological findings (adenocarcinoma vs others), maximum tumour dimension, C/T ratio (≥0.5 vs <0.5), preoperative CEA titre, maximum SUVmax in the primary tumour and smoking status (pack-years, ≥20 vs <20). The factors that were potentially associated with false results in the univariate analysis were also evaluated by a multivariate analysis. *P*-values of <0.05 were considered to be significant.

In addition to the above analyses, the diagnostic efficacy of FDG-PET according to four cut-off values of SUVmax in the primary tumour (≥3, ≥5, ≥7 and ≥10) was calculated with respect to sensitivity, specificity, accuracy and positive and negative predictive value (PPV and NPV) for the patients with pathological N1–2 disease. We added a supplementary explanation that these cut-off values, especially 5, 7 and 10, of SUVmax in the primary tumour were found as prognostic factors or relapse-factors of NSCLC here and there in several previous reports from Cerfolio *et al.* [7] and Downey *et al.* [8]. Therefore, we determined these cut-off values including 5, 7 and 10 in this study.

# RESULTS

One hundred and fifty-nine (60.0%) of the patients were men and 106 (40.0%) were women (Table 1). The median age was 68 years, with a range of 35–89 years. One hundred and fifty-two patients had a smoking history. Among them, 133 patients were heavy smokers of >20 pack-years. Histological findings were as follows; adenocarcinoma in 202 (75.5%), squamous cell carcinoma in 51 (19.2%), large cell neuroendocrine carcinoma in seven (2.6%), adenosquamous carcinoma in three (1.1%) and other in two (0.8%). Clinical staging was IA (T1aN0M0, T1bN0M0) in 191 (72.1%), IB (T2aN0M0) in 50 (18.9%), IIA (T2bN0M0) in nine (3.4%), IIB (T3N0M0) in 13 (4.9%) and IIIA (T4N0M0) in two (0.7%). In clinical IIB, the main tumour invaded the parietal pleura, chest wall and superior vena cava. Similarly, in clinical IIIA, the main tumour directly invaded the trachea. Among all of the clinical N0 NSCLC patients, 214 (80.8%) had pathological N0 status and 51 (20.1%) had pathological nodal involvement. The median SUVmax in the primary tumour was 3.8, with a range of 0.6–44.1. The median maximum tumour dimension and preoperative CEA titre were 23.0 mm (range 5–96 mm) and 2.9 (range 0.4–80.5), respectively.

The correlation between clinicopathological features including the findings by FDG-PET and pathological nodal involvement were investigated (Table 2). No significant correlations were seen between clinicopathological features and pathological nodal involvement, except for histological findings, maximum tumour dimension, C/T ratio and SUVmax in the primary tumour. Among the 201 patients with adenocarcinoma, only 32 (15.9%) had pathological nodal involvement, while 19 (29.7%) of the remaining 64 with non-adenocarcinoma had pathological nodal involvement ($P = 0.019$). Among the 45 patients with a C/T ratio <0.5, only one (2.2%) had pathological nodal involvement, while 50 (22.7%) of the remaining 220 with a C/T ratio ≥0.5 had pathological nodal involvement ($P < 0.001$). There were significant differences in maximum tumour dimension and SUVmax in the primary tumour between pathological N0 and N1–2 ($P = 0.012$

**Table 1:** Overall patient characteristics

| Clinicopathological features | Number of patients |
|---|---|
| Overall | 265 |
| Gender | |
| Male/female | 159/106 |
| Age | |
| Range (median) | 35–89 (68) |
| Smoking, pack-years | |
| <20/≥20 | 132/133 |
| Pathological nodal involvement | |
| pN0/N1/N2 | 214/27/24 |
| Histological findings | |
| Adenocarcinoma | 202 (76.2%) |
| Squamous cell carcinoma | 51 (19.2%) |
| Large cell neuroendocrine carcinoma | 7 (2.6%) |
| Adenosquamous carcinoma | 3 (1.1%) |
| Other[a] | 2 (0.7%) |
| Tumour size (mm) | |
| Range (median) | 5.0–96.0 (23.0) |
| Preoperative CEA titre | |
| Range (median) | 0.4–80.5 (2.9) |
| Clinical stage | |
| IA | 191 (72.1%) |
| IB | 50 (18.9%) |
| IIA | 9 (3.4%) |
| IIB | 13 (4.9%) |
| IIIA | 2 (0.7%) |
| SUVmax in the primary tumour | |
| Range (median) | 0.6–44.1 (3.8) |

[a]Carcinoid: 1, pleomorphic carcinoma: 1.
CEA: carcinoembryonic antigen; SUVmax: maximum standardized uptake value.

**Table 2:** Correlations between clinicopathological features and pathological nodal involvement

| Variables | pN0 ($n$ = 214) | pN1–2 ($n$ = 51) | $P$-value[a] |
|---|---|---|---|
| Age,[b] mean | 62.3 (±9.8) | 66.1 (±10.1) | 0.20 |
| Gender (male/female) | 124/90 | 35/16 | 0.20 |
| Histological findings (adenocarcinoma/other) | 169/45 | 32/19 | 0.019 |
| Tumour size[b] (mm), mean | 25.2 (±13.8) | 30.8 (±15.3) | 0.012 |
| Preoperative CEA titre,[b] mean | 5.3 (±9.6) | 8.3 (±12.8) | 0.064 |
| C/T ratio (<0.5/≥0.5) | 44/170 | 1/50 | <0.001 |
| SUVmax in the primary tumour,[b] mean | 5.4 (±5.6) | 9.6 (±5.5) | <0.001 |
| Pack-year smoking (<20/≥20) | 112/102 | 20/31 | 0.12 |

[a]$P$-value in logistic regression analysis.
[b]Continuous variable.
CEA: carcinoembryonic antigen; SUVmax: maximum standardized uptake value; C/T ratio: ratio of consolidation to tumour dimension.

and $P < 0.001$). NSCLC with pathological nodal involvement were larger and had higher uptake values than those without pathological nodal involvement. The preoperative CEA titre in pathological N0 status tended to be higher than that in pathological N1–2 disease, but this difference was not significant.

**Table 3:** Univariate analysis for factors that predicted pathological nodal involvement

| Variables | Odds ratio | 95% CI | $P$-value[a] |
|---|---|---|---|
| Age[b] | 0.988 | 0.958–1.109 | 0.44 |
| Gender, male | 1.588 | 0.828–3.044 | 0.16 |
| Histological findings, non-adenocarcinoma | 2.230 | 1.157–4.279 | 0.018 |
| Preoperative CEA titre[b] | 1.022 | 0.997–1.048 | 0.081 |
| Tumour size[b] (mm) | 1.025 | 1.005–1.045 | 0.014 |
| C/T ratio, ≥0.5 | 12.941 | 1.739–96.317 | 0.012 |
| SUVmax in the primary tumour[b] | 1.115 | 1.058–1.174 | <0.001 |
| Pack-year smoking, ≥20 | 1.702 | 0.913–3.173 | 0.094 |

[a]$P$-value in logistic regression analysis.
[b]Continuous variable.
CI: confidence interval; CEA: carcinoembryonic antigen; SUVmax: maximum standardized uptake value; C/T ratio: ratio of consolidation to tumour dimension.

The univariate analysis revealed four factors that may be associated with pathological nodal involvement in clinical N0 NSCLC. Histological findings, maximum tumour dimension and C/T ratio (≥0.5) on the preoperative CT scan and SUVmax of the primary tumour were all significant predictors ($P$ = 0.018, 0.014, 0.012 and <0.001) (Table 3). Preoperative CEA titre did not predict pathological nodal disease in this study ($P$ = 0.081).

The factors that were potentially associated with false results in a univariate analysis, histological findings, maximum tumour dimension and C/T ratio (≥0.5) on preoperative CT scan and SUVmax of the primary tumour, were also evaluated by a multivariate analysis. The multivariate analysis showed that both the C/T ratio (≥0.5) on preoperative CT scan and SUVmax of the primary tumour were independent predictive factors for pathological nodal involvement ($P$ = 0.046 and 0.016) (Table 4).

The sensitivity, specificity, accuracy, PPV and NPV of pathological N1–2 disease are shown in Table 5. Among patients with NSCLC who had an SUVmax for FDG-PET of 10 or more, the sensitivity, specificity, accuracy, PPV and NPV of mediastinal node involvement were 49.0, 83.2, 76.6, 41.0 and 87.3%, respectively. In patients with an SUVmax in the primary tumour of 10 or more, the PPV was higher than those in the three other populations (≥3, ≥5 and ≥7). Among the 61 patients with NSCLC who had an SUVmax for FDG-PET of 10 or more, 25 (41.0%) had pathological N1–2 disease, while only 26 (12.7%) of the remaining 204 patients with an SUVmax for FDG-PET of <10 had nodal disease ($P < 0.0001$).

## DISCUSSION

Pathological nodal involvement is a very important prognostic factor in patients with potentially resectable NSCLC. Several authors have reported that induction chemotherapy and chemoradiotherapy followed by surgery could provide pathological down-staging and better long-term survival in patients with N2 disease [9–11]. Therefore, the accurate preoperative evaluation of mediastinal nodes is important for planning NSCLC treatment [11].

In Japan, the conventional clinical staging regimen for NSCLC does not include FDG-PET. CT scan is routinely used for preoperative diagnosis and locoregional staging for lung cancer. The clinical criterion of mediastinal lymph node involvement is a short dimension of 10 mm or more on CT scan. A diagnosis of hilar lymph node involvement requires the presence of swollen soft tissue on CT scan. Thus, the clinical diagnosis of lymph node is on the basis of lymph node enlargement. However, obstructive pneumonia, atelectasis, infection by nontuberculous mycobacteria and interstitial pneumonia can also cause swollen lymph nodes [1]. On the other hand, a metastatic node can appear to have a normal size. These conditions could lead to false-positive and false-negative results, which could result in stage-migration of resectable lung cancer [2–4, 12].

FDG-PET is now widely used for the clinical staging of NSCLC [7, 11, 13–17]. The first approved indications for the staging of NSCLC by the use of FDG-PET were reported in the 1990s [18]. Since 2001, the combination of PET and CT) has rapidly eclipsed stand-alone PET [19]. Furthermore, it has been reported that the diagnostic value of PET-CT for the preoperative staging of NSCLC was superior to that of CT alone [1, 7, 15–20]. Previous randomized trials have proven that PET-CT is significantly more accurate and more sensitive for the staging of NSCLC than the conventional staging regimen [21]. Additionally, the addition of PET-CT examination has been shown to reduce the frequency of futile thoracotomies. However, PET-CT examination was not associated with improved overall survival in patients with NSCLC [21]. Previous reports have shown that potential lymph node involvement may not be detected by FDG-PET. In our study, 51 (19.2%) of 265 patients with clinical N0 NSCLC had pathological lymph node involvement, which was comparable to the findings in previous reports (5.7–25%) [2–4, 7]. This population, especially those with N2 disease, could receive futile thoracotomies and show reduced overall survival in each clinical stage.

Several authors have reported that CEA titre, maximum tumour size, C/T ratio and tumour disappearance rate (TDR) on HRCT scan were each good clinical predictors of pathological nodal involvement [22, 23]. In addition, these factors could also be prognostic determinants for NSCLC [24].

In this study, the C/T ratio on preoperative CT scan significantly predicted pathological nodal involvement. However, preoperative CEA titre was not a significant predictor.

In this study, in a univariate analysis, histological findings predicted pathological nodal involvement. In particular, squamous cell carcinoma was seen in many cases of pathological N1–2 disease, compared with adenocarcinoma. Eighteen (35.3%) of 51 patients with squamous cell carcinoma had pathological N1–2 disease, while only 32 (15.8%) of 202 patients with adenocarcinoma had pathological N1–2 disease. Thirty nine (76.4%) of 51 patients with squamous cell carcinoma were heavy smokers (>40 pack-years). Their lungs were subjected to emphysematous change and this was believed to be the basis of poorly differentiated carcinoma. All of the cases of squamous cell carcinoma were invasive carcinoma with a C/T ratio of ≥0.5 on preoperative CT scan. Additionally, the median SUVmax of primary squamous cell carcinoma was 11.0, with a range of 2–25.5. Thus, clinical N0 squamous cell carcinoma had a high potential for pathological nodal disease in this study. Further studies on squamous cell carcinoma will be needed in the future.

The tumour size was limited to that which tended to be associated with lymph node involvement. This was the reason why we excluded small-sized lung carcinoma that showed pure GGO with both a C/T ratio of 50% or less and a maximum tumour dimension of 2 cm or less on chest CT scan. On the other hand, including patients with tumour as small as 5 mm might also impact on this analysis, therefore these very small tumours were at the detection limit of this method.

Additionally, the clinical strategy for pathological N2 disease is controversial. As noted above, pathological N2 patients with clinical N0 NSCLC might be subjected to futile thoracotomies. On the other hand, the presence of pathological N1 disease could lead to unavoidable changes in. For example, it may become necessary to convert usual lobectomy to bilobectomy, sleeve lobectomy or double sleeve lobectomy. Therefore, an accurate staging for resectable NSCLC is very valuable for not only patients but also surgeons. In this study, in all of the cases of pathological N1–2 disease among clinical N0 NSCLC patients, the main tumour showed a strong uptake value of SUVmax, compared with pathological N0 disease (Table 5). The PPV of

**Table 4:** Multivariate analysis for factors that predicted pathological nodal involvement

| Variables | Odds ratio | 95% CI | *P*-value[a] |
|---|---|---|---|
| Histological findings, non-adenocarcinoma | 1.001 | 1.458–2.186 | 0.99 |
| Tumour size[b] (mm) | 1.005 | 0.980–1.030 | 0.72 |
| C/T ratio, ≥0.5 | 7.950 | 1.034–61.128 | 0.046 |
| SUVmax in the primary tumour[b] | 1.085 | 1.015–1.159 | 0.016 |

[a]*P*-value in logistic regression analysis.
[b]Continuous variable.
CI: confidence interval; SUVmax: maximum standardized uptake value.

**Table 5:** The correlation between SUVmax in the primary tumour and pathological N12 disease in overall patients

| SUVmax | cN0 | cN0-pN1-2 | Sensitivity | Specificity | Accuracy | PPV | NPV |
|---|---|---|---|---|---|---|---|
| ≥3 | 155 | 46 | 90.1 | 49.1 | 57.0 | 29.7 | 95.5 |
| ≥5 | 114 | 36 | 70.6 | 64.9 | 64.9 | 31.6 | 90.1 |
| ≥7 | 89 | 31 | 60.9 | 69.7 | 70.1 | 34.8 | 88.6 |
| ≥10 | 61 | 25 | 49.0 | 83.2 | 76.6 | 41.0 | 87.3 |

SUVmax: maximum standardized uptake value; PPV: positive predictive value; NPV: negative predictive value.

pathological N1–2 disease with clinical N0 NSCLC that showed an SUVmax in the primary tumour of 10 or more was 41.0%. On the other hand, the PPV of pathological N1–2 disease that showed an SUVmax in the primary tumour of ≥3, ≥5 or ≥7 were 29.7, 31.6 and 34.8%, respectively. In the case of an SUVmax in the primary tumour of 10 or more, over 40% of clinical N0 patients could have occult nodal metastasis. Meanwhile, it was previously reported that the patients without an enlarged lymph node and a PET-negative mediastinum may proceed directly to surgery [16]. Moreover, it was reported that radical lymphandectomy could be omitted in patients with stage I NSCLC tumour <1 cm or SUVmax 2.0 [25]. However, each of these studies was retrospective and did not consider SUVmax of the primary tumour. On the basis of the results of our study, further preoperative modality such as EBUS-TBNA or mediastinoscopy could be considered for the accurate clinical staging of patients with NSCLC, and particularly in those who show a strong uptake value of SUVmax.

In conclusion, the pathological nodal status in clinical N0 NSCLC was significantly predicted by SUVmax for FDG-PET of the primary tumour instead of the lymph nodes themselves. In particular, patients with NSCLC who show a strong uptake value of SUVmax could have occult pathological nodal metastases, and may be indicated for a further preoperative modality for accurate clinical staging. For these reasons, FDG-PET is a feasible modality for the clinical staging of NSCLC.

## Funding

This work was supported in part by a Grant-in-Aid for Cancer Research from the Ministry of Health, Labour and Welfare, Japan.

**Conflict of interest**: none declared.

## REFERENCES

[1] Konishi J, Yamazaki K, Tsukamoto E, Tamaki N, Onodera Y, Otake T *et al.* Mediastinal lymph node staging by FDG-PET in patients with non-small cell lung cancer: analysis of false-positive FDG-PET findings. Respiration 2003;70:500–6.

[2] Al-Sarraf N, Aziz R, Gately K, Lucey J, Wilson L, McGovern E *et al.* Pattern and predictors of occult mediastinal lymph node involvement in non-small cell lung cancer patients with negative mediastinal uptake on positron emission tomography. Eur J Cardiothorac Surg 2008;33:104–9.

[3] Melek H, Gunluoglu MZ, Demir A, Akin H, Olcmen A, Dincer SI. Role of positron emission tomography in mediastinal lymphatic staging of non-small cell lung cancer. Eur J Cardiothorac Surg 2008;33:294–9.

[4] Carnochan FM, Walker WS. Positron emission tomography may underestimate the extent of thoracic disease in lung cancer patients. Eur J Cardiothorac Surg 2009;35:781–4; discussion 84–5.

[5] Suzuki K, Koike T, Asakawa T, Kusumoto M, Asamura H, Nagai K *et al.* A prospective radiological study of thin-section computed tomography to predict pathological noninvasiveness in peripheral clinical IA lung cancer (Japan Clinical Oncology Group 0201). J Thorac Oncol 2011;6:751–6.

[6] Suzuki K, Kusumoto M, Watanabe S, Tsuchiya R, Asamura H. Radiologic classification of small adenocarcinoma of the lung: radiologic-pathologic correlation and its prognostic impact. Ann Thorac Surg 2006;81:413–9.

[7] Cerfolio RJ, Bryant AS, Ohja B, Bartolucci AA. The maximum standardized uptake values on positron emission tomography of a non-small cell lung cancer predict stage, recurrence, and survival. J Thorac Cardiovasc Surg 2005;130:151–9.

[8] Downey RJ, Akhurst T, Gonen M, Vincent A, Bains MS, Larson S *et al.* Preoperative F-18 fluorodeoxyglucose-positron emission tomography maximal standardized uptake value predicts survival after lung cancer resection. J Clin Oncol 2004;22:3255–60.

[9] Rosell R, Gomez-Codina J, Camps C, Maestre J, Padille J, Canto A *et al.* A randomized trial comparing preoperative chemotherapy plus surgery with surgery alone in patients with non-small-cell lung cancer. N Engl J Med 1994;330:153–8.

[10] Bueno R, Richards WG, Swanson SJ, Jaklitsch MT, Lukanich JM, Mentzer SJ *et al.* Nodal stage after induction therapy for stage IIIA lung cancer determines patient survival. Ann Thorac Surg 2000;70:1826–31.

[11] De Leyn P, Lardinois D, Van Schil PE, Rami-Porta R, Passlick B, Zielinski M *et al.* ESTS guidelines for preoperative lymph node staging for non-small cell lung cancer. Eur J Cardiothorac Surg 2007;32:1–8.

[12] Takamochi K, Yoshida J, Murakami K, Niho S, Ishii G, Nishimura M *et al.* Pitfalls in lymph node staging with positron emission tomography in non-small cell lung cancer patients. Lung Cancer 2005;47:235–42.

[13] Gomez-Caro A, Garcia S, Reguart N, Arguis P, Sanchez M, Gimferrer JM *et al.* Incidence of occult mediastinal node involvement in cN0 non-small-cell lung cancer patients after negative uptake of positron emission tomography/computer tomography scan. Eur J Cardiothorac Surg 2010;37:1168–74.

[14] Tasci E, Tezel C, Orki A, Akin O, Falay O, Kutlu CA. The role of integrated positron emission tomography and computed tomography in the assessment of nodal spread in cases with non-small cell lung cancer. Interact CardioVasc Thorac Surg 2010;10:200–3.

[15] Sanli M, Isik AF, Zincirkeser S, Elbek O, Mete A, Tuncozgur B *et al.* Reliability of positron emission tomography-computed tomography in identification of mediastinal lymph node status in patients with non-small cell lung cancer. J Thorac Cardiovasc Surg 2009;138:1200–5.

[16] Fischer BM, Mortensen J, Hansen H, Vilmann P, Larsen SS, Loft A *et al.* Multimodality approach to mediastinal staging in non-small cell lung cancer. Faults and benefits of PET-CT: a randomised trial. Thorax 2011; 66:294–300.

[17] Gupta NC, Graeber GM, Bishop HA. Comparative efficacy of positron emission tomography with fluorodeoxyglucose in evaluation of small (<1 cm), intermediate (1–3 cm), and large (>3 cm) lymph node lesions. Chest 2000;117:773–8.

[18] McCann J. New techniques catch lung cancers earlier. J Natl Cancer Inst 1997;89:1838–9.

[19] Beyer T, Townsend DW, Brun T, Kinahan PE, Charron M, Roddy R *et al.* A combined PET/CT scanner for clinical oncology. J Nucl Med 2000;41: 1369–79.

[20] Lardinois D, Weder W, Hany TF, Kamel EM, Korom S, Seifert B *et al.* Staging of non-small-cell lung cancer with integrated positron-emission tomography and computed tomography. N Engl J Med 2003;348: 2500–7.

[21] *Fischer B, Lassen U, Mortensen J, Larsen S, Loft A, Bertelsen A et al.* Preoperative staging of lung cancer with combined PET-CT. N Engl J Med 2009;361:32–9.

[22] Takamochi K, Nagai K, Yoshida J, Suzuki K, Ohde Y, Nishimura M *et al.* Pathologic N0 status in pulmonary adenocarcinoma is predictable by combining serum carcinoembryonic antigen level and computed tomographic findings. J Thorac Cardiovasc Surg 2001;122:325–30.

[23] Takamochi K, Nagai K, Suzuki K, Yoshida J, Ohde Y, Nishiwaki Y. Clinical predictors of N2 disease in non-small cell lung cancer. Chest 2000;117: 1577–82.

[24] Takamochi K, Yoshida J, Nishimura M, Yokose T, Sasaki S, Nishiwaki Y *et al.* Prognosis and histologic features of small pulmonary adenocarcinoma based on serum carcinoembryonic antigen level and computed tomographic findings. Eur J Cardiothorac Surg 2004;25:877–83.

[25] Casiraghi M, Travaini LL, Maisonneuve P, Tessitore A, Brambilla D, Agoglia BG *et al.* Lymph node involvement in T1 non-small-cell lung cancer: could glucose uptake and maximal diameter be predictive criteria? Eur J Cardiothorac Surg 2011;39:e38–43.

Interactive CardioVascular and Thoracic Surgery Advance Access published December 17, 2012

Interactive CardioVascular and Thoracic Surgery (2012) 1–5
doi:10.1093/icvts/ivs520

ORIGINAL ARTICLE



# Lung cancer with scattered consolidation: detection of new independent radiological category of peripheral lung cancer on thin-section computed tomography

Takeshi Matsunaga, Kenji Suzuki*, Aritoshi Hattori, Mariko Fukui, Yoshitaka Kitamura, Yoshikazu Miyasaka, Kazuya Takamochi and Shiaki Oh

Division of General Thoracic Surgery, Juntendo University School of Medicine, Bunkyo-ku, Tokyo, Japan

* Corresponding author. Division of General Thoracic Surgery, Juntendo University School of Medicine, 1-3 Hongo, 3-chome, Bunkyo-ku, Tokyo 113-8431, Japan. Tel: +81-3-38133111; fax: +81-3-58000281; e-mail: kjsuzuki@juntendo.ac.jp (K. Suzuki).

Received 13 August 2012; received in revised form 9 November 2012; accepted 15 November 2012

## Abstract

**OBJECTIVES**: Ground glass opacity (GGO) on thin-section computed tomography (CT) has been reported to be a favourable prognostic marker in lung cancer, and the size or area of GGO is commonly used for preoperative evaluation. However, it can sometimes be difficult to evaluate the status of GGO.

**METHODS**: A retrospective study was conducted on 572 consecutive patients with resected lung cancer of clinical stage IA between 2004 and 2011. All patients underwent preoperative CT and their radiological findings were reviewed. The areas of consolidation and GGO were evaluated for all lung cancers. Lung cancers were divided into three categories on the basis of the status of GGO: GGO, part solid and pure solid. Lung cancers in which it was difficult to measure GGO were selected and their clinicopathological features were investigated.

**RESULTS**: Seventy-one (12.4%) patients had lung cancer in whom it was difficult to measure GGO. In all these cases, consolidation and GGO were not easily measured because of their scattered distribution. In this cohort, nodal metastases were not observed at all. The frequency of other pathological factors, such as lymphatic and/or vascular invasion, was significantly lower ($P < 0.0001$).

**CONCLUSIONS**: This new category of lung cancer with scattered consolidation on thin-section CT scan tended to be pathologically less invasive. When lung cancer has GGO and is difficult to measure because of a scattered distribution, its prognosis could be favourable regardless of the area of GGO. This new category could be useful for the preoperative evaluation of lung cancer.

**Keywords:** Lung cancer • Thoracic surgery • Diagnosis • Lymph node • Ground glass opacity

## INTRODUCTION

Small-sized lung cancer tends to be found in screening with computed tomography (CT). CT can detect not only small tumours but also tumours that are faint on chest roentgenogram, such as tumours with ground glass opacity (GGO). GGO on thin-section CT is one of the most favourable prognostic factors in lung cancer. In most previous reports, the size of GGO has been evaluated in one dimension for predicting the prognosis [1–10]. These authors have claimed that the proportion of GGO and consolidation was important for predicting the prognosis, and their findings were confirmed by a prospective multi-institutional trial (JCOG0201) [4]. On the other hand, it is often difficult to measure the dimension of GGO or consolidation. In this study, we investigated the clinicopathological features of lung cancer with a GGO appearance that was difficult to measure on thin-section CT scan to aid in determining the optimal management.

## MATERIALS AND METHODS

### Study population

A retrospective study was conducted on 1179 patients with primary lung cancer, which was resected between January 2004 and April 2011 at our institute. Among them, 637 patients had clinical stage IA lung cancer, and thin-section CT was available for 572. Clinical stage IA was defined as follows: (1) primary tumor was 3 cm or less in greatest dimension, (2) there was no regional lymph node metastasis and distant metastasis, according to the 7th edition of the Union International Contre le Cancer TNM staging system. Thin-section CT was performed to evaluate the entire lung with collimation of 1–2 mm. The lung was photographed with a window level of −500 to −700 Hounsfield units (HU) and a window width of 1500–2000 HU as a lung window.

## Definition of lung cancer with scattered consolidation (LCSC)

All thin-section CT scans were reviewed by 3 of the authors (T.M., K.S. and K.T.), and the following radiological factors were investigated: maximum tumour dimension, maximum dimension of consolidation, distribution of GGO and pleural tail. The ratio of consolidation to tumour size was evaluated. We defined LCSC as follows:

(1) lung cancer with consolidation that is difficult to be measured on thin-section CT scan (Fig. 1),
(2) lung cancer with GGO whose distribution is scattered. In all these cases, consolidation and GGO were not easily measured because of discontinuous consolidation of tumour. So these tumours have more than two parts of consolidation with >1 mm.
(3) We exclude tumours with emphysematous lung because some of these areas of consolidation seem to be discontinuous. We investigated the clinicopathological features of LCSC and compared them with those of other types of lung cancer. We also determined the category to which LCSC had originally belonged. Our classification of GGO consisted of three types: GGO, part solid and pure solid. Conventional classification is based on the findings on thin-section CT scan, i.e. the consolidation/tumour ratio (CTR). The GGO, part solid and pure solid groups were defined as tumour having a CTR of ≤0.5, >0.5 and 1.0, respectively. Finally, we divided all the lung cancers into four categories, i.e. the three conventional categories and the new category of LCSC.

## Statistical analysis

To compare two factors, the $\chi^2$ test or Fisher's exact test was used. Multivariate analyses were performed by logistic regression analysis. A *P*-value of <0.05 was considered to be statistically significant. All statistical calculations were performed using SPSS.

# RESULTS

## Characteristics of lung cancer with scattered consolidation

LCSC was observed in 71 (12%) of 572 patients. The clinicopathological features of these patients were compared according to radiological findings (Table 1). There were 29 men and 42 women who ranged in age from 24 to 86 years (median 66 years). Compared with other tumours, the LCSCs were significantly bigger in the maximum tumour dimension. Women tended to have LCSC, and the CTR was ≥0.5 in more than half of the patients with LCSC, but this difference was not statistically significant. All the LCSCs were histologically adenocarcinomas and showed pathological invasiveness, such as nodal metastasis, or lymphatic or vascular invasion, and these differences were statistically significant ($P < 0.0001$).

## Relationship between conventional ground glass opacity status and lung cancer with scattered consolidation

The relationships between the three conventional categories and LCSC are shown in Table 2. None of the patients in the pure solid group was categorized as LCSC. LCSC was found in the part solid and GGO groups, significantly more often than in the pure solid group. With regard to pathological invasiveness, the conventional GGO, part solid and pure solid groups showed 0, 5.9 and 25.0% nodal metastasis, respectively (Table 3). For other forms of invasiveness, such as lymphatic or vascular invasion, there were significant relationships between these pathological factors and conventional GGO status.

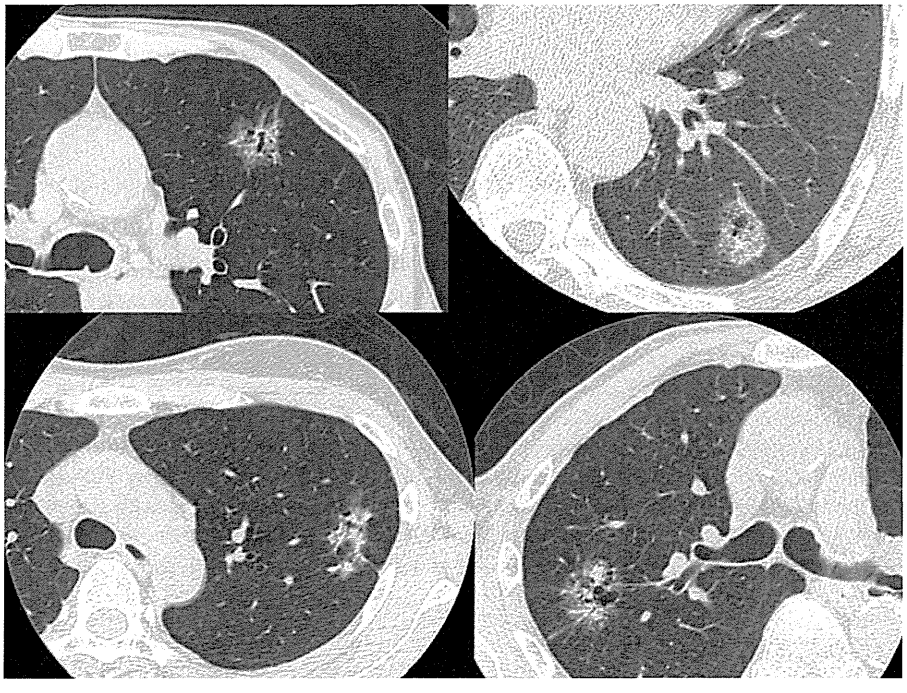

**Figure 1:** The proportions of consolidation and ground glass opacity were not easily measured because of their scattered distribution such as in these cases.

**Table 1:** Clinicopathological features by radiological findings

| Clinicopathological factors | LCSC | Others | *P*-value[a] |
|---|---|---|---|
| Gender | | | |
| Men | 29 (40.8%) | 247 (49.3%) | 0.1820 |
| Women | 42 (59.2%) | 254 (50.7%) | |
| Age | | | |
| Years (median) | 66 (24-86) | 66 (26-89) | 0.4508 |
| Smoking states (pack-year) | | | |
| ≥40 | 11 (11.3%) | 113 (23.5%) | 0.2142 |
| <40 | 55 (88.7%) | 368 (76.5%) | |
| CEA (ng/ml) | | | |
| ≥5.0 | 7 (10.4%) | 89 (18.1%) | 0.1657 |
| <5.0 | 60 (89.6%) | 402 (81.9%) | |
| Tumour size (mm) | | | |
| 20 | 38 (53.5%) | 329 (65.7%) | 0.0458 |
| <20 | 33 (42.5%) | 172 (34.3%) | |
| Visual CTR | | | |
| <0.5 | 25 (35.2%) | 126 (25.1%) | 0.0719 |
| ≥0.5 | 46 (64.8%) | 375 (74.9%) | |
| Histology | | | |
| Adenocarcinoma | 71 (100%) | 430 (85.8%) | <0.0001 |
| Others | 0 (0%) | 71 (14.2%) | |
| Pathological N status | | | |
| N0 | 71 (100%) | 424 (84.8%) | <0.0001 |
| N1 or 2 | 0 (0%) | 76 (15.2) | |
| Lymphatic invasion | | | |
| Positive | 12 (16.9%) | 235 (46.9%) | <0.0001 |
| Negative | 59 (83.1%) | 266 (53.1%) | |
| Vascular invasion | | | |
| Positive | 5 (7.0%) | 213 (42.5%) | <0.0001 |
| Negative | 66 (93.0%) | 288 (57.5%) | |

[a]$\chi^2$-test or Fisher's exact test.
LCSC: lung cancer with scattered consolidation; CEA: carcinoembryonic antigens; CTR: consolidation tumour ratio.

**Table 2:** The relationship between ground glass appearance and lung cancer with scattered consolidation

| Conventional category | LCSC | non-LCSC | *P*-value[a] |
|---|---|---|---|
| GGO group (CTR ≤ 0.5) | 25 (35.2%) | 126 (25.1%) | <0.0001 |
| Part solid group (0.5 < CTR < 1.0) | 46 (64.8%) | 106 (21.2%) | |
| Pure solid group (CTR = 1) | 0 (0%) | 269 (53.7%) | |

[a]Fisher's exact test.
GGO: ground glass opacity; CTR: consolidation tumour ratio.

**Table 3:** The relationship between conventional categories and p-N status

| Conventional category | p-N1 or 2 | p-N0 | *P*-value[a] |
|---|---|---|---|
| GGO group (CTR ≤ 0.5) | 0 (0%) | 151 (100%) | <0.0001 |
| Part solid group (0.5 < CTR < 1) | 9 (5.9%) | 143 (94.1%) | |
| Pure solid group (CTR = 1) | 67 (25.0%) | 201 (75.0%) | |

[a]Fisher's exact test.
GGO: ground glass opacity; CTR: consolidation tumour ratio.

**Table 4:** Results of multivariate analysis for predictors of lymphatic invasion

| Variables | Hazard ratio | 95% CI | *P*-value[a] |
|---|---|---|---|
| LCSC (vs non-LCSC) | 0.208 | 0.100-0.433 | <0.0001 |
| Gender (male) | 1.584 | 1.055-2.378 | 0.0264 |
| CEA (≥5 ng/ml) | 3.033 | 1.744-5.274 | <0.0001 |
| Tumour size (>20 mm) | 2.520 | 1.647-3.855 | <0.0001 |
| Visual CTR (≥0.5) | 16.414 | 7.724-34.883 | <0.0001 |

[a]*P*-value in logistic regression analysis.
CI: confidence interval; LCSC: lung cancer with scattered consolidation; CEA: carcinoembryonic antigens; CTR: consolidation tumour ratio.

**Table 5:** Incidence of nodal metastasis and lymphatic invasion according to a new radiological grouping

| *New category* | pN | Ly | *P*-value[a] |
|---|---|---|---|
| GGO group (CTR ≤ 0.5) | 0/126 (0%) | 7/126 (5.5%) | <0.0001 |
| LCSC group | 0/71 (0%) | 12/71 (16.9%) | |
| Part solid group (0.5 < CTR < 1) | 9/106 (8.5%) | 41/106 (38.7%) | |
| Pure solid group (CTR = 1) | 67/268 (25.0%) | 187/268 (69.5%) | |

[a]Fisher's exact test.
pN: pathological nodal metastasis; Ly: lymphatic invasion; GGO: ground glass opacity; CTR: consolidation tumour ratio; LCSC: lung cancer with scattered consolidation.

## Predictors of pathological invasiveness

In a multivariate analysis for predictors of lymphatic and vascular invasion, the new category LCSC was an independent predictor along with gender, the preoperative serum CEA titer, maximum tumour dimension and CTR (Table 4). LCSC showed pathological invasiveness more often than GGO, but less often than part solid lung cancer. LCSC did not show lymph node metastasis (Table 5).

## DISCUSSION

As CT is used more widely, we increasingly have opportunities to detect small or faint lung nodules that could be diagnosed as lung cancer. Although lobectomy is now a standard operation based on the results of LCSG [11], limited resection such as wide wedge resection or segmentectomy has been studied in many institutions [12-15]. Many surgeons think that limited resection could be equivalent to lobectomy for appropriately selected patients.

**Table 6:** Meta-analysis on GGO as a prognostic factor for lung cancer

| Authors/year | No. | Cases | Methods | Good prognosis | Study design |
|---|---|---|---|---|---|
| Jang/1996 [9] | 14 | - | - | Focal area of GGO | Retrospective |
| Suzuki/2000 [7] | 69 | Ad, cIA | CTR | GGO > 0.5 | Retrospective |
| Aoki/2001 [1] | 127 | 3 cm | CTR | GGO > 0.5 | Retrospective |
| Takamochi/2001 [8] | 269 | Ad | TDR | TDR and CEA | Retrospective |
| Kim/2001 [10] | 224 | Ad, cIA | Visual | GGO extent | Retrospective |
| Okada/2003 [3] | 167 | Ad, 3 cm | TDR | TDR > 0.5 | Retrospective |
| Ohde/2003 [2] | 98 | Ad, 2 cm | CTR | GGO > 0.5 | Retrospective |
| Suzuki/2006 [6] | 349 | Ad, 2 cm | CTR | CTR and CEA | Retrospective |
| Suzuki/2011 [4] | 811 | Ad, 3 cm | CTR | CTR < 0.25 | Prospective |

GGO: ground glass opacity; CTR: consolidation tumour ratio; Ad: adenocarcinoma; TDR: tumour shadow disappearance rate.

Preoperative GGO on thin-section CT has been reported to be a favourable prognostic factor (Table 6) [1–10, 16–18]. The preoperative GGO status is important for selecting patients who are suitable for limited surgical resection [19–22]. While most authors have evaluated GGO in terms of the maximum tumour size and consolidation in one dimension, there is still some controversy regarding the optimal methods for the evaluation of ground glass. It is not uncommon for lung cancers to show GGO that is difficult to measure. Thus, we identified the clinicopathological characteristics of this type of lung cancer.

None of the patients with LCSC was in the pure GGO or pure solid group. There were more women than men in the LCSC group, but this difference was not statistically significant. Generally, men are more likely to have lung cancer, and the observed predominance of women could mean that this type of lung cancer is not related to smoking status or that carcinogenesis could be associated with gender. Tumours in LCSC were significantly larger than those in the other groups ($P = 0.0458$). LCSC shows atypical radiological findings on thin-section CT, and thus, a preoperative diagnosis could be difficult. This is one of the reasons for the larger size of LCSC. LCSC tends to grow slowly, which makes diagnosis difficult. All the LCSCs were histologically adenocarcinoma, and this is a distinct characteristic of LCSC.

LCSC did not show nodal metastases. LCSC tends to be less invasive pathologically, such as with regard to lymphatic or vascular invasion. One of the most potent prognostic factors is the size or nature of a central fibrosis of adenocarcinoma of the lung [7, 12, 23, 24]. Active fibroblasts in the central fibrosis have been reported to be associated with a poor prognosis [23]. Active fibroblasts are a sign of destruction of the basement membrane by cancer cells, which leads to mesenchymal destruction of the lung. This destruction results in the exclusion of air in the lung. This is a phase of consolidation on CT scan. If the invasion or destruction of the mesenchyme of the lung is minimal, air in the lung remains within the lung cancer, resulting in a ground glass appearance on thin-section CT. Thus, consolidation on thin-section CT could be strongly associated with the invasiveness of lung cancer [4]. According to the above considerations, LCSC has no pure consolidation and its pathological invasiveness should be minimal. When LCSC grows, it should show pure consolidation and could metastasize to nodes and distant organs. So an early diagnosis is necessary.

LCSC is a new radiological entity for lung cancer. This category is included mainly in the part-solid group. It is difficult to measure the size of consolidation for LCSC, which makes classification of this tumour vague. Similar radiological findings for lung cancer have been reported as part-solid groups [6]. However, this is the first report to focus on this category of lung cancer. JCOG0201 defined peripheral early lung cancer to be lung cancer of ≤2.0 cm in size in which consolidation is less than one fourth of the maximum tumour dimension [4]. Most of these lesions could be cured with limited surgical resection [13–15, 25]. LCSC should also be curable by limited surgical resection, although a clinical trial is needed to support this supposition. This study was limited in that it was a retrospective study in a single institute and the sample size was small. Thus, we are planning to perform a prospective multicentre trial in the near future to collect more patients with lung cancer having scattered consolidation.

In conclusion, the new category lung cancer with scattered consolidation has been proposed, and recognition of this category could resolve the problem of misclassification of lung cancer with difficult-to-measure consolidation on thin-section CT. Limited surgical resection may be the preferred option for lung cancers in this category in the near future.

## ACKNOWLEDGEMENTS

This study was supported in part by a Grant-in-Aid for Cancer Research from the Ministry of Health, Labour and Welfare of Japan.

**Conflict of interest:** none declared.

## REFERENCES

[1] Aoki T, Tomoda Y, Watanabe H, Nakata H, Kasai T, Hashimoto H *et al.* Peripheral lung adenocarcinoma: correlation of thin-section CT findings with histologic prognostic factors and survival. Radiology 2001;220: 803–9.

[2] Ohde Y, Nagai K, Yoshida J, Nishimura M, Takahashi K, Suzuki K *et al.* The proportion of consolidation to ground-glass opacity on high resolution CT is a good predictor for distinguishing the population of non-invasive peripheral adenocarcinoma. Lung Cancer 2003;42:303–10.

[3] Okada M, Nishio W, Sakamoto T, Uchino K, Tsubota N. Discrepancy of computed tomographic image between lung and mediastinal windows as a prognostic implication in small lung adenocarcinoma. Ann Thorac Surg 2003;76:1828–32.
[4] Suzuki K, Koike T, Asakawa T, Kusumoto M, Asamura H, Nagai K *et al.* A prospective radiological study of thin-section computed tomography to predict pathological noninvasiveness in peripheral clinical IA lung cancer (Japan Clinical Oncology Group 0201). J Thorac Oncol 2011;6: 751–6.
[5] Suzuki K, Koike T, Asamura H, Nagai K. Radiologic-pathologic correlation in stage IA adenocarcinoma of the lung. *Proceedings of ASCO 2006;* Chicago.
[6] Suzuki K, Kusumoto M, Watanabe S, Tsuchiya R, Asamura H. Radiologic classification of small adenocarcinoma of the lung: radiologic-pathologic correlation and its prognostic impact. Ann Thorac Surg 2006; 81:413–9.
[7] Suzuki K, Yokose T, Yoshida J, Nishimura M, Takahashi K, Nagai K *et al.* Prognostic significance of the size of central fibrosis in peripheral adenocarcinoma of the lung. Ann Thorac Surg 2000;69:893–7.
[8] Takamochi K, Nagai K, Yoshida J, Suzuki K, Ohde Y, Nishimura M *et al.* Pathologic N0 status in pulmonary adenocarcinoma is predictable by combining serum carcinoembryonic antigen level and computed tomographic findings. J Thorac Cardiovasc Surg 2001;122:325–30.
[9] Jang HJ, Lee KS, Kwon OJ, Rhee CH, Shim YM, Han J. Bronchioloalveolar carcinoma: focal area of ground-glass attenuation at thin-section CT as an early sign. Radiology 1996;199:485–8.
[10] Kim EA, Johkoh T, Lee KS, Han J, Fujimoto K, Sadohara J *et al.* Quantification of ground-glass opacity on high-resolution CT of small peripheral adenocarcinoma of the lung: pathologic and prognostic implications. AJR Am J Roentgenol 2001;177:1417–22.
[11] Ginsberg RJ, Rubinstein LV. Randomized trial of lobectomy versus limited resection for T1 N0 non-small cell lung cancer. Lung Cancer Study Group. Ann Thorac Surg 1995;60:615–22.
[12] Travis WD, Brambilla E, Noguchi M, Nicholson AG, Geisinger KR, Yatabe Y *et al.* International association for the Study of Lung Cancer/American Thoracic Society/European Respiratory Society international multidisciplinary classification of lung adenocarcinoma. J Thorac Oncol 2011;6: 244–85.
[13] Okada M, Koike T, Higashiyama M, Yamato Y, Kodama K, Tsubota N. Radical sublobar resection for small-sized non-small cell lung cancer: a multicenter study. J Thorac Cardiovasc Surg 2006;132:769–75.
[14] Yoshikawa K, Tsubota N, Kodama K, Ayabe H, Taki T, Mori T. Prospective study of extended segmentectomy for small lung tumors: the final report. Ann Thorac Surg 2002;73:1055–8.
[15] El-Sherif A, Gooding WE, Santos R, Pettiford B, Ferson PF, Fernando HC *et al.* Outcomes of sublobar resection versus lobectomy for stage I non-small cell lung cancer: a 13-year analysis. Ann Thorac Surg 2006;82: 408–15.
[16] Ost DE, Gould MK. Decision making in patients with pulmonary nodules. Am J Respir Crit Care Med 2012;185:363–72.
[17] Armato SG 3rd, McNitt-Gray MF, Reeves AP, Meyer CR, McLennan G, Aberle DR *et al.* The Lung Image Database Consortium (LIDC): an evaluation of radiologist variability in the identification of lung nodules on CT scans. Acad Radiol 2007;14:1409–21.
[18] Chen S, Suzuki K, MacMahon H. Development and evaluation of a computer-aided diagnostic scheme for lung nodule detection in chest radiographs by means of two-stage nodule enhancement with support vector classification. Med Phys 2011;38:1844–58.
[19] Watanabe S, Watanabe T, Arai K, Kasai T, Haratake J, Urayama H. Results of wedge resection for focal bronchioloalveolar carcinoma showing pure ground-glass attenuation on computed tomography. Ann Thorac Surg 2002;73:1071–5.
[20] Yamato Y, Tsuchida M, Watanabe T, Aoki T, Koizumi N, Umezu H *et al.* Early results of a prospective study of limited resection for bronchioloalveolar adenocarcinoma of the lung. Ann Thorac Surg 2001;71:971–4.
[21] Yoshida J, Ishii G, Yokose T, Aokage K, Hishida T, Nishimura M *et al.* Possible delayed cut-end recurrence after limited resection for ground-glass opacity adenocarcinoma, intraoperatively diagnosed as Noguchi type B, in three patients. J Thorac Oncol 2010;5:546–50.
[22] Yoshida J, Nagai K, Yokose T, Nishimura M, Kakinuma R, Ohmatsu H *et al.* Limited resection trial for pulmonary ground-glass opacity nodules: fifty-case experience. J Thorac Cardiovasc Surg 2005;129:991–6.
[23] Noguchi M, Morikawa A, Kawasaki M, Matsuno Y, Yamada T, Hirohashi S *et al.* Small adenocarcinoma of the lung. Histologic characteristics and prognosis. Cancer 1995;75:2844–52.
[24] Shimosato Y, Suzuki A, Hashimoto T, Nishiwaki Y, Kodama T, Yoneyama T *et al.* Prognostic implications of fibrotic focus (scar) in small peripheral lung cancers. Am J Surg Pathol 1980;4:365–73.
[25] Tsubota N, Ayabe K, Doi O, Mori T, Namikawa S, Taki T *et al.* Ongoing prospective study of segmentectomy for small lung tumors. Study Group of Extended Segmentectomy for small lung tumor. Ann Thorac Surg 1998;66:1787–90.

Human Cancer Biology

Clinical Cancer Research

# Upregulation of Notch2 and Six1 Is Associated with Progression of Early-Stage Lung Adenocarcinoma and a More Aggressive Phenotype at Advanced Stages

Takahiro Mimae[1,2], Morihito Okada[1], Man Hagiyama[2,3], Yoshihiro Miyata[1], Yasuhiro Tsutani[1], Takao Inoue[3], Yoshinori Murakami[2], and Akihiko Ito[3]

## Abstract

**Purpose:** Lung adenocarcinoma often manifests as tumors with mainly lepidic growth. The size of invasive foci determines a diagnosis of *in situ*, minimally invasive adenocarcinoma, or invasive types and suggests that some adenocarcinomas undergo malignant progression in that order. This study investigates how transcriptional aberrations in adenocarcinoma cells at the early stage define the clinical phenotypes of adenocarcinoma tumors at the advanced stage.

**Experimental Design:** We comprehensively searched for differentially expressed genes between preinvasive and invasive cancer cells in one minimally invasive adenocarcinoma using laser capture microdissection and DNA microarrays. We screened expression of candidate genes in 11 minimally invasive adenocarcinomas by reverse transcriptase PCR and examined their involvement in preinvasive-to-invasive progression by transfection studies. We then immunohistochemically investigated the presence of candidate molecules in 64 samples of advanced adenocarcinoma and statistically analyzed the findings, together with clinicopathologic variables.

**Results:** The transcription factors *Notch2* and *Six1* were upregulated in invasive cancer cells in all 11 minimally invasive adenocarcinomas. Exogenous Notch2 transactivated *Six1* followed by *Smad3*, *Smad4*, and *vimentin*, and enlarged the nuclei of NCI-H441 lung epithelial cells. Immunochemical staining for the transcription factors was double positive in the invasive, but not in the lepidic growth component of a third of advanced Ads, and the disease-free survival rates were lower in such tumors.

**Conclusions:** Paired upregulation of *Notch2* and *Six1* is a transcriptional aberration that contributes to preinvasive-to-invasive adenocarcinoma progression by inducing epithelial–mesenchymal transition and nuclear atypia. This aberration persisted in a considerable subset of advanced adenocarcinoma and conferred a more malignant phenotype on the subset. *Clin Cancer Res; 18(4); 945–55. ©2011 AACR.*

## Introduction

Adenocarcinoma is the most widespread histologic subtype of lung cancer in most countries, accounting for almost half of all lung cancers (1). Lung adenocarcinomas, especially advanced tumors, rarely comprise a single histologic component, and more than 90% of lung adenocarcinomas are of the mixed subtype according to the 2004 WHO classification (2). In an effort to address the complex histologic heterogeneity of adenocarcinomas, a new classification has recently been proposed (3). According to it, a small tumor with the lepidic growth pattern is diagnosed as either adenocarcinoma *in situ* or minimally invasive adenocarcinoma, depending on the presence or absence of microinvasion ($\leq$ 5 mm). If a microinvasion focus of a minimally invasive adenocarcinoma becomes overt (overt invasion; > 5mm), the tumor will be then diagnosed as lepidic-predominant invasive adenocarcinoma. As might be predicted from these diagnostic criteria, to clearly distinguish between adenocarcinoma *in situ* and minimally invasive adenocarcinoma, as well as between minimally invasive adenocarcinoma and lepidic-predominant invasive adenocarcinoma can be difficult. Rather, it seems reasonable to consider that a significant subset of these 3 subtypes is biologically serial and that each subtype represents a different stage of adenocarcinoma progression.

The concept of progression from adenocarcinoma *in situ* to minimally invasive adenocarcinoma is widely accepted (4–9). Noguchi and colleagues noted 2 types of small

**Authors' Affiliations:** [1]Surgical Oncology, Division of Genome Radiobiology and Medicine, Programs for Biomedical Research, Graduate School of Biomedical Sciences, Hiroshima University, Hiroshima; [2]Division of Molecular Pathology, Institute of Medical Science, University of Tokyo, Tokyo; and [3]Department of Pathology, Faculty of Medicine, Kinki University, Osaka, Japan

**Note:** Supplementary data for this article are available at Clinical Cancer Research Online (http://clincancerres.aacrjournals.org/).

**Corresponding Author:** Akihiko Ito, Department of Pathology, Faculty of Medicine, Kinki University, 377-2 Ohno-Higashi, Osaka-Sayama, Osaka 589-8511, Japan. Phone: 81-72-366-0221; Fax: 81-72-360-2028; E-mail: aito@med.kindai.ac.jp

**doi:** 10.1158/1078-0432.CCR-11-1946

## Translational Relevance

Lung adenocarcinomas with mainly lepidic growth component are diagnosed as *in situ*, minimally invasive adenocarcinoma, or lepidic-predominant invasive adenocarcinoma types, depending on the size of invasive foci. In a minimally invasive adenocarcinoma, differentially expressed genes were comprehensively searched between the preinvasive and invasive components, and 2 transcriptional factors, *Notch2* and *Six1*, were identified as genes upregulated in the invasive component in all 11 minimally invasive adenocarcinomas examined. Transfection experiments suggested that Notch2 and Six1 cooperatively induced epithelial–mesenchymal transition of adenocarcinoma cells. Clinicopathologic analyses revealed that upregulation of both Notch2 and Six1 in invasive foci was detected in one-third of 64 lepidic-predominant invasive adenocarcinomas, and these tumors represented an aggressive phenotype. Paired upregulation of *Notch2* and *Six1* seemed to occur during preinvasive-to-invasive adenocarcinoma progression and define a more malignant subset of advanced adenocarcinoma. Notch2 and Six1 are not only useful biomarkers for malignant potential of adenocarcinoma but also can be therapeutic targets in adenocarcinoma.

(maximum diameter, < 2 cm) adenocarcinomas. These are type A (adenocarcinoma *in situ* according to the 2011 classification) that consists entirely of neoplastic cells that grow in lepidic growth pattern and type C (minimally invasive adenocarcinoma according to the 2011 classification) that consists of peripheral lepidic growth and a central microinvasion focus. The 2 types of tumors differ clinicopathologically. (i) After complete resection, patients with type A have 100% disease-specific survival, whereas the 5-year survival rate for patients with type C is 75% (9). (ii) Type C tumors have higher rates of p53 positivity, proliferation, and nuclear atypia than type A (8, 10, 11). Interpreting these data based on the 2011 classification, the microinvasion focus of minimally invasive adenocarcinoma is considered to develop due to the malignant progression of noninvasive, *in situ* neoplastic cells of the lepidic growth component. In contrast to the development of type C or minimally invasive adenocarcinoma tumors, the progression of minimally invasive adenocarcinoma to more advanced forms, including lepidic-predominant invasive adenocarcinoma, has not been studied in detail.

Genetic studies of adenocarcinoma progression have found mutations in *KRAS* and *EGFR* at the preinvasive stage, such as atypical adenomatous hyperplasia and adenocarcinoma *in situ* (12–15), and some adenocarcinomas have the amplification of these genes at the later stage of invasion and metastasis (7, 16, 17). Besides such genomic alterations, specific transcriptional pathways seem to become upregulated during the progression of adenocarcinoma, because recent findings have increasingly clarified that lung cancer progression is promoted by epithelial–mesenchymal transition (EMT; ref. 18) that is controlled by a group of transcription factors that includes Slug, which is a zinc finger type (19). The homeobox transcription factors Oct4 and downstream Nanog both function upstream of Slug to promote EMT in A549 lung adenocarcinoma cells (20). Although lung adenocarcinoma progression is assumed to be a stepwise process triggered by multiple genetic aberrations, which aberration(s) accounts for each process in the stepwise progression requires precise examination.

In this study, we attempted to obtain the genetic evidence, indicating that all or a subset of lepidic-predominant invasive adenocarcinoma develops from minimally invasive adenocarcinoma, and to clarify what clinical phenotypes the subset has. For this purpose, we designed the experiments that were composed of 3 parts. In the first part, we aimed to comprehensively compare the gene expression profiles between lepidic growth and microinvasion cancer cells from a single minimally invasive adenocarcinoma and successfully identified 2 transcription factors *Notch2* and *Six1* as genes upregulated in microinvasion cells. In the second part, we examined whether the identified genes might play causative roles in early-stage adenocarcinoma progression from lepidic growth to microinvasion cells, and found that Notch2 and Six1 coordinately induced EMT and nuclear atypia in lung epithelial cells. Finally in the third part, we immunohistochemically stained 64 specimens of lepidic-predominant invasive adenocarcinoma for Notch2 and Six1 and found that a third were a simple advanced form of minimally invasive adenocarcinoma, judging from the upregulation of Notch2 and Six1 in overt invasion cells. Importantly, the disease-free survival of patients with such tumors was poorer.

## Materials and Methods

### Sample selection

This study included patients with both consolidated lung tumors and ground glass opacities on chest high-resolution computed tomography images who underwent lobectomy or segmentectomy at Hiroshima University Hospital between 2007 and 2010 (Hiroshima, Japan). All patients provided written, informed consent to participate in this study and our Institutional Review Board approved the protocol (approval number: Hi-29). Half of the cancerous tissues were placed in Ultramount Aqueous Permanent Mounting Medium (DakoCytomation) and frozen for later studies, whereas the other half was preserved in 10% formalin for diagnosis. Gene expression was analyzed in samples of minimally invasive adenocarcinoma from 11 patients and 64 lepidic-predominant invasive adenocarcinoma tumor samples were immunohistochemically stained.

### Cell culture

NCI-H441 human lung papillary adenocarcinoma cells, A549 human lung adenocarcinoma cells and MDA-MB-231

human breast cancer cells were purchased from the American Type Culture Collection and RERF-LC-MS human lung adenocarcinoma cells were from Japanese Cancer Research Resources Bank (JCRB, Osaka, Japan) in 2010, and all experimentation using cell lines proceeded within 6 months after resuscitation. NCI-H441 cells and A549 cells were grown in RPMI-1640 (Nacalai Tesque) and Dulbecco's Modified Eagle Medium (Nacalai Tesque) supplemented with 10% FBS, antibiotics containing 100 units/mL penicillin, 100 μg/mL streptomycin (Invitrogen), and 0.01M-HEPES buffer (Nacalai Tesque) at 37°C in 5% $CO_2$/95% air. RERF-LC-MS cells were grown in Eagle's minimal essential medium (Nacalai Tesque) supplemented with 10% FBS, antibiotics, and 0.1 mmol/L nonessential amino acids (GIBCO-Invitrogen) at 37°C in 5% $CO_2$/95% air. MDA-MB-231 cells were grown in L-15 (Sigma-Aldrich) medium supplemented with 10% FBS, antibiotics, and 0.3 g/L L-glutamine (Sigma-Aldrich) at 37°C in 100% air.

### Laser capture microdissection

Serial 15-μm sections of the 11 frozen minimally invasive adenocarcinoma tumors were stained with hematoxylin. Only cancer cells were selectively and separately collected from the lepidic growth and microinvasion components using laser capture microdissection (LMD7000; Leica Microsystems GmbH). The cancer cells were placed in the caps of collection tubes containing Tris [2-carboxyethyl] phosphine hydrochloride buffer. The collection time for one slide was 30 minutes. Twenty slides were done for each component. Each cell pool was frozen with dry ice immediately after collection.

### RNA purification and amplification with Cy3 or Cy5 labeling

Total RNA was extracted from each cell pool using NucleoSpin RNA XS (Macherey-Nagel GmbH & Co. KG) and from one small ($\leq$ 1 cm) minimally invasive adenocarcinoma tumor and then cDNAs and amino allyl aRNA were synthesized from the RNA using Amino Allyl MessageAmp II aRNA Amplification Kits (Applied Biosystems). CyeDye coupling and fragmentation proceeded according to a protocol supplied by Toray Industries Inc. The concentration, purity, and integrity of the amplified and labeled aRNA were determined using a Eukaryotes Total RNA Nano Series II (Agilent Technologies). Total RNA from cultured cells was also extracted using NucleoSpin RNA XS.

### Gene microarray analysis

Amplified RNA samples from microinvasion components were analyzed using 3D-Gene Human Oligo chip 25k (Toray Industries Inc.) microarrays of 25,370 distinct genes and RNA samples from lepidic growth components as controls. The 3-dimensional microarrays were constructed with wells as spaces between probes and cylinder stems with 70-mer oligonucleotide probes on the top to promote efficient hybridization. Cy3- or Cy5-labeled aRNA pools in hybridization buffer were hybridized for 16 hours according to the supplier's protocol (www.3d-gene.com). Hybridization signals were scanned using ScanArray Express Scanner (PerkinElmer) and processed using GenePixPro version 5.0 (Molecular Devices). Signals detected for each gene were normalized by global normalization (Cy3/Cy5 ratio median = 1) and Cy3/Cy5 normalized ratios >2.0 or <0.5 were, respectively, defined as commonly upregulated or downregulated genes.

### Semiquantitative reverse transcriptase PCR

We analyzed the expression of *Notch2*, *Six1*, *thyroid transcription factor-1* (*TTF-1*), *Smad3*, *Smad4*, *vimentin*, *E-cadherin*, and *GAPDH* mRNA using reverse transcriptase PCR (RT-PCR) using SuperScriptTMIII First-Strand Synthesis SuperMix (Invitrogen) for the RT. In brief, total RNA was incubated with 50 ng of random hexamer primers and 1 μL of annealing buffer at 65°C for 5 minutes. The RNA was then incubated at 25°C for 5 minutes and at 50°C for 50 minutes in a final volume of 20 μL of reaction mixture containing 1× first-strand reaction mix comprising 5 mmol/L $MgCl_2$, 0.5 mmol/L of each deoxynucleotide triphosphate (dNTP), and 2 μL of SuperScriptTMIII/RNaseOUTTM Enzyme Mix.

The cDNA constructs were amplified by PCR using TaKaRa Ex Taq (Takara). The PCR conditions were 35 cycles of 30 seconds at 94°C (denaturation), 30 seconds at 55°C (annealing), and 30 seconds at 72°C (extension). The sense and antisense primers were 5′-AAAAATGGGGCCAACCGAGAC-3′ and 5′-TTCATCCAGAAGGCGCACAA-3′ for human *Notch2*, 5′-ACTCTCTGCTCGGCCCCCTC-3′ and 5′-AAGGCTGCTGAAACAGGCGT-3′ for human *Six1*, 5′-ATGTCGATGAGTCCAAAG-3′ and 5′-TCACCAGGTCCGA-3′ for human *TTF-1*, 5′-CGGGCCATGGAGCTGTGTGA-3′ and 5′-ACCTGCGTCCATGCTGTGGT-3′ for human *Smad3*, 5′-TCAGGGCCTCAGCCAGGACA-3′ and 5′-TCTCCTCCAGAAGGGTCCACGT-3′ for human *Smad4*, 5′-CAAGGGCCAAGGCAAGTCGC-3′ and 5′-GCCGTGAGGTCAGGCTTGGA-3′ for human *vimentin*, 5′-CCCTGGCTTTGACGCCGAGA-3′ and 5′-AAACGGAGGCCTGATGGGGC-3′ for human *E-cadherin*, and 5′-ACCACAGTCCATGCCATCAC-3′ and 5′-TCCACCACCCTGTTGCTGTA-3′ for human *GAPDH*, respectively. The PCR products were resolved by electrophoresis on 1% agarose gels, stained with ethidium bromide, and densitometrically analyzed. The RT-PCR signal intensity was quantified using ImageJ software (NIH) to compare *Notch2*, *Six1*, *TTF-1*, *Smad3*, *Smad4*, *vimentin*, *E-cadherin*, and *GAPDH* mRNA levels.

### Construction of plasmid vectors expressing Notch2 intracellular domain, TTF-1, and siRNA against Six1

The cDNA construct for Notch2 intracellular domain (ICD; amino acids 1,703–2,475) inserts was amplified by PCR using KOD FX DNA polymerase (Toyobo Co. Ltd.) with following primer set: sense, 5′-CCGGATCCATGAAGCGTAAG-3′ (containing the first codon of Notch2 ICD); antisense, 5′-CCGTTAACTCACGCATAAACCTG-3′ (containing the stop codon of Notch2 ICD). The *TTF-1* gene produces 2 alternative transcripts, of which the short form consists of more than 90% of the total transcripts (21). The open reading frame of the short form of the cDNA from

NCI-H441 cells was amplified by PCR using the primer set: sense, 5′-CCGAATTCATGTCGATGAGTCCAAAG-3′; antisense, 5′-CCGTTAACTCACCAGGT-CCGA-3′. The PCR products were resolved by electrophoresis on 1% agarose gels and stained with ethidium bromide. Targeted bands were excised from gels and DNA was extracted and purified using the Wizard SV Gel and PCR Clean-Up System (Promega Corporation), as described by the manufacturer. Extracted DNA chains were annealed and ligated into the *Bam*HI/*Hpa*I (for Notch2) and *Eco*RI/*Hpa*I (for TTF-1) sites of pCX4-bsr, a modified pCX-bsr retroviral vector (22) provided by Dr. T. Akagi (Osaka Bioscience Institute, Osaka, Japan), and sequenced.

The pSilencer4.1-CMVneo siRNA plasmid vector (Ambion) was used to construct pSilencer4.1-CMVneo-si-Six1 and the negative control, pSilencer4.1-CMVneo-scramble. A DNA chain with the following sense and antisense sequences was synthesized to target the Six1 sequence: 5′-GATCCCCAGCTCAGAAGAGGAATTTTC-AAGAGAAA-TTCCTCTTCTGAGCTGGTT-3′ (sense) and 5′-AGCTTAACCAGCTCAGAAGAGGAATT-TCTCTTGAA-AATTCCTCTTCTGAGCTGGG-3′ (antisense). The target sequence of the negative control (scramble-pSilencer4.1-CMVneo) was 5′-GATCCCGT-CGATTTTGTGATGCTCG-TCAGTTCAAGAGACTGACGAGCATCACAAAATCGACG-G-TT-3′ (sense) and 5′-AGCTTAACGTCGATTTTGTGA-TGCTCGTCAGTCTCTTGAACTGA-CGAGCATCACAAAAT-CGACGG-3′ (antisense), which has no homology with any human DNA. The DNA chains were annealed and ligated into the *Bam*HI/*Hin*dIII sites of pSilencer4.1-CMVneo to generate pSilencer4.1-CMVneo-si-Six1. The negative control pSilencer4.1-CMVneo-scramble vector was constructed in the same manner. The plasmids were extracted and the accuracy of the constructs was confirmed by sequencing.

### Transfection

NCI-H441 cells were transiently transfected with empty pCX4-bsr, pCX4-bsr-Notch2 ICD, or pCX4-bsr-TTF-1 using FuGENE 6 (Roche Applied Science). In brief, $2.0 \times 10^5$ cells were seeded on 60-mm culture dishes overnight until 50% to 80% confluence was reached. Serum-free medium (194 μL) and 6.0 μL of FuGENE 6 reagent were mixed in 1.5-mL tubes and incubated for 5 minutes at room temperature. Plasmid vectors (2.0 μg each) were added and the contents were mixed and incubated with transfection reagent and DNA complex for at least 15 minutes at room temperature. The transfection reagent and DNA complex were added drop wise to the cultured cells and incubated for 48 hours. The medium was removed and the cells were rinsed 3 times with PBS. The transfected cells were then used in various experiments. A549, RERF-LC-MS, and MDA-MB-231 were also transiently transfected with empty pCX4-bsr or pCX4-bsr-Notch2 ICD using FuGENE 6.

Double transfection proceeded as follows. NCI-H441 cells were transiently transfected with 2.0 μg of each of pCX4-bsr-Notch2 ICD and the empty pSilencer4.1-CMVneo, or pSilencer4.1-CMVneo-scramble, or pSilencer4.1-CMVneo -si-Six1 using FuGENE 6.

### Immunohistochemistry

Tissues fixed with 10% formalin were embedded in paraffin and cut into 4-μm thick sections that were deparaffinized, rehydrated, and autoclaved for 20 minutes at 121°C in 10 mmol/L citrate buffer (pH 6.0) and then incubated in methanol containing 3% peroxide for 5 minutes. The sections were washed 3 times with PBS between all steps of the procedure. Nonspecific Ig binding in the sections was blocked by incubation with PBS containing 2% bovine serum albumin (BSA) for 10 minutes. The sections were then incubated with anti-Notch2 antibody (ab8926, 1:400 dilution; Abcam) and/or anti-Six1 antibody (HPA001893, 1:100 dilution; Sigma-Aldrich) in PBS containing 2% BSA for 2 hours at room temperature, followed by horseradish peroxidase–conjugated anti-rabbit Ig G antibody (1:100 dilution; Santa Cruz) in PBS containing 2% BSA for 2 hours at 4°C. Color was developed using aminoethylcarbazole (DAB; Dako) as the substrate for peroxidase. Tissues were counterstained with hematoxylin and mounted. Negative immunohistochemical control procedures comprised the omission and replacement of primary antibodies with appropriate concentrations of normal rabbit or mouse IgG. Slides were examined using a light microscope (BX51; Olympus) equipped with a CCD camera DP72 (Olympus). The results on the control slides were negative.

Cancer cells were deemed positive for Notch2 when the cytoplasm of over half of the cancer cells in each of the lepidic growth and microinvasion components was intensely stained. Other staining profiles were defined as negative. Cancer cells were deemed positive for Six1 when nuclei in over half of the cancer cells in each of the lepidic growth and microinvasion components were intensely stained. Other staining profiles were defined as negative.

### Nuclear size analysis

Five minimally invasive adenocarcinoma tumors that contained a Notch2-negative lepidic growth component and a Notch2-positive microinvasion component were immunohistochemically selected. The greatest nuclear dimension of cancer cells in both the lepidic growth and microinvasion components was separately determined in 5 tumors using hematoxylin and eosin (H&E) staining and light microscopy (BX51). The greatest nuclear dimension of 200 cells was measured in random fields for each component from each tumor. The greatest nuclear dimension of the control and of NCI-H441 cells transfected *in vitro* with empty pCX4-bsr, pCX4-bsr-Notch2 ICD, or pCX4-bsr-TTF-1 was assessed by nuclear staining using 4′,6-diamino-2-phenylindole (DAPI) and the fluorescence microscope, Axio Observer D1 (Carl Zeiss). We determined the nuclear dimensions of 100 cells in randomly selected fields in 3 independent experiments.

### Statistical analysis

Data about signal intensity and cell morphology are described as means ± SD or as means ± SE and were analyzed using Student *t* test. The clinicopathologic findings were analyzed using the Mann–Whitney *U* test for

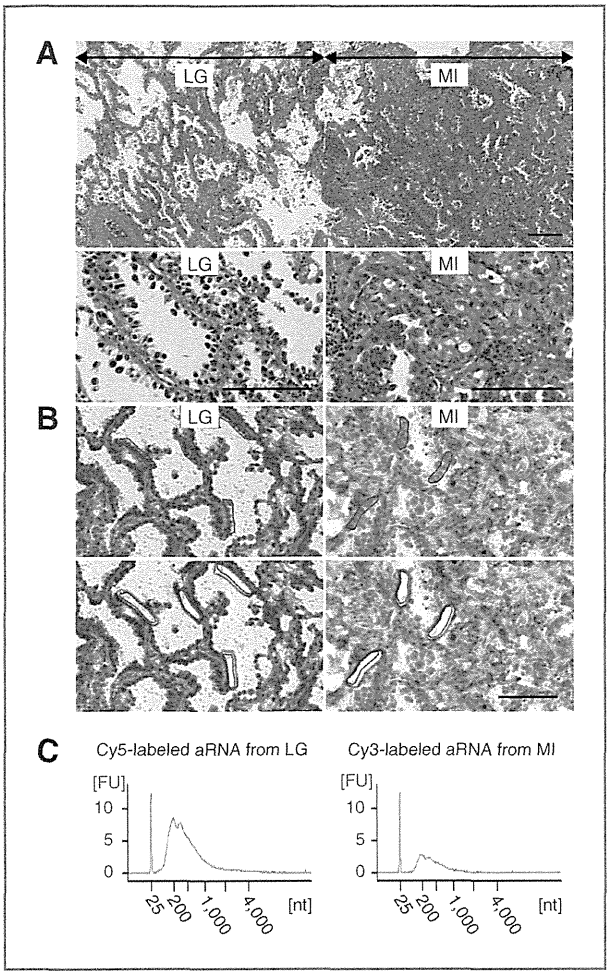


Figure 1. Laser capture microdissection of lepidic growth (LG) and microinvasion (MI) cancer cells from a single minimally invasive adenocarcinoma (case 1) and probe preparation for DNA microarray analysis. A, photomicrograph of minimally invasive adenocarcinoma from case 1 stained with H&E. Top, low-power field view (original magnification, ×100) containing both lepidic growth and microinvasion components; bottom, high-power field view (original magnification, ×400) of each component. B, lepidic growth and microinvasion cancer cells collected by laser capture microdissection from frozen sections of minimally invasive adenocarcinoma tumor. Cancer cells circled in red (top) were cut out using laser pulses run along the circles (bottom). C, verification of aRNA probes for DNA microarray analysis. Total RNA extracted from pools of lepidic growth and microinvasion cancer cells served as templates for preparation of aRNA probes. Quality and quantities of probes were verified by resolving Cy3- or Cy5-labeled aRNA by capillary gel electrophoresis. The amounts of RNA extracted and amplified were 46.2 ng and 14.3 μg for lepidic growth component and 48.4 ng and 4.0 μg for microinvasion component, respectively. Bar, 100 μm.

continuous variables and $\chi^2$ tests for categorical variables. Disease-free survival (DFS) curves were calculated using the Kaplan–Meier method. Univariate and multivariate analyses were done using the log-rank and logistic regression tests, respectively. A $P$ value of $\leq 0.05$ was regarded as significant.

## Results

### Isolation of genes that are differentially expressed in lepidic growth and microinvasion cancer cells in a single minimally invasive adenocarcinoma

A small (1 cm in greatest dimension), solitary lung tumor was surgically resected and histopathologically diagnosed as minimally invasive adenocarcinoma (formerly, type C by Noguchi classification; Fig. 1A; case 1 in Fig. 2A and Supplementary Table S1). We separately isolated lepidic growth and microinvasion cancer cells without contamination from frozen tumor sections using a laser capture microdissection system (Fig. 1B). We extracted total RNAs from about 500 lepidic growth and microinvasion cancer cells and then amplified and labeled the RNAs using T7 RNA polymerase. Fig. 1C shows the amounts and quality of the original total RNAs and amplified aRNAs. The aRNAs were comparatively analyzed using highly sensitive oligo DNA microarrays. The complete gene expression dataset of the microdissected minimally invasive adenocarcinoma specimen is available at Gene Expression Omnibus (GEO) accession number GSE30663 (23). The numbers of genes whose expression levels were double or more and half or less in the microinvasion cancer cells were 2,905 and 2,143, respectively. Supplementary Table S2 shows the top 30 of each of

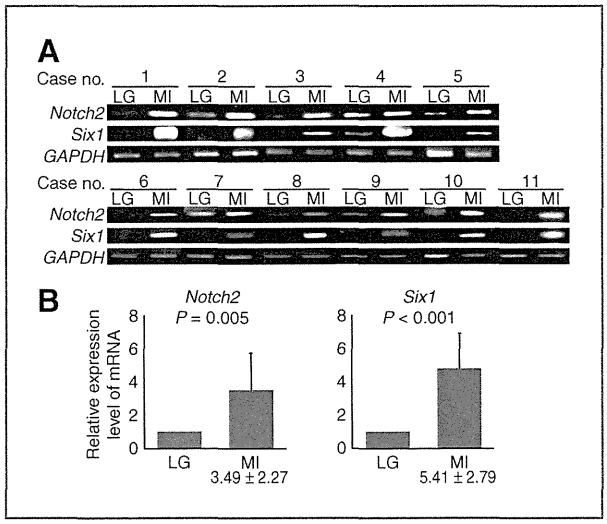


Figure 2. RT-PCR analyses of *Notch2* and *Six1* in total RNA from lepidic growth (LG) and microinvasion (MI) cancer cells in 11 minimally invasive adenocarcinomas. lepidic growth and microinvasion cancer cells were separately collected from frozen sections of minimally invasive adenocarcinomas (cases 1 to 11 listed in Supplementary Table S1) using laser capture microdissection. Total RNAs were extracted from each cell pool and analyzed by RT-PCR using primer sets for *Notch2*, *Six1*, or *GAPDH*. Portions of PCR products were resolved by electrophoresis on 1% agarose gels (A). All band intensities were converted to densitometric values; *Notch2* and *Six1* values were normalized to that of *GAPDH* and then means and SD of 11 minimally invasive adenocarcinomas were calculated. Expression levels of *Notch2* and *Six1* mRNA in microinvasion cancer cells are expressed as relative values normalized to 1 for means in lepidic growth cancer cells (B).

the upregulated (>94-fold) and downregulated (<1/25.4-fold) candidate genes.

### Upregulation of Notch2 and its downstream Six1 in microinvasion cancer cells

We found that *Six1* (136-fold) was the most upregulated among the top 30 genes in microinvasion cancer cells, and *Notch2* was 10.7-fold upregulated in the complete dataset. We considered that this paired upregulation was worthy of further investigation because both Six1 and Notch2 can function as transcription factors and Six1 is a putative downstream target of Notch2 (24, 25). As with minimally invasive adenocarcinoma from case 1, we extracted total RNAs from lepidic growth and microinvasion cancer cells separately from minimally invasive adenocarcinomas resected from cases 2 to 11 (Fig. 2A and Supplementary Table S1). *Six1* and *Notch2* mRNA expression was then screened in all 11 minimally invasive adenocarcinomas by semiquantitative RT-PCR. Significantly more mRNA for either gene was found in microinvasion than in lepidic growth cancer cells from all 11 minimally invasive adenocarcinomas (Fig. 2A and B). The expression of Notch2 and Six1 proteins was examined in the case 10 minimally invasive adenocarcinoma by immunohistochemistry. Notch2 and Six1 immunoreactive signals were clearly detected in the cytoplasm and nucleus of microinvasion cancer cells, respectively, whereas lepidic growth component cells were nearly completely negative for the two molecules (Fig. 3).

We speculated whether Notch2 upregulation results in *Six1* transactivation in lung epithelial cells and examined this notion in NCI-H441 cells that have been widely studied as lung epithelial cells. The results of RT-PCR analyses revealed that these cells expressed endogenously undetectable levels of *Notch2* or *Six1* (Fig. 4A, lane 1). Because Notch2 is enzymatically processed to release its ICD that functions as a transcription factor (26), we subcloned Notch2 ICD cDNA into the mammalian expression vector, pCX4-bsr. NCI-H441 cells transfected with this plasmid contained not only abundant exogenous transcripts for Notch2 ICD but also abundant endogenous transcripts for Six1 (Fig. 4A, lane 3 and Supplementary Fig. S1). We also transfected NCI-H441 cells with the cDNA for TTF-1, well known as a lung epithelial transcription factor, but *Six1* transactivation was undetectable (Fig. 4A, lane 4 and Supplementary Fig. S1). Similar experiments using MDA-MB-231 breast cancer cells that express endogenously detectable levels of *Notch2* and *Six1* showed that exogenous Notch2 ICD did not upregulate, but rather slightly downregulated *Six1* (Fig. 4A, lanes 8–10). These results suggested that Notch2 specifically transactivates *Six1* in NCI-H441.

### Involvement of Notch2 and Six1 in EMT and nuclear atypism in lung epithelial cells

Notch2 and Six1 promote EMT in various cancers partly through activating the TGF-β intracellular signaling pathways that involve the intracellular signal transducers Smad3 and Smad4 (27–29). Consistent with their epithelioid

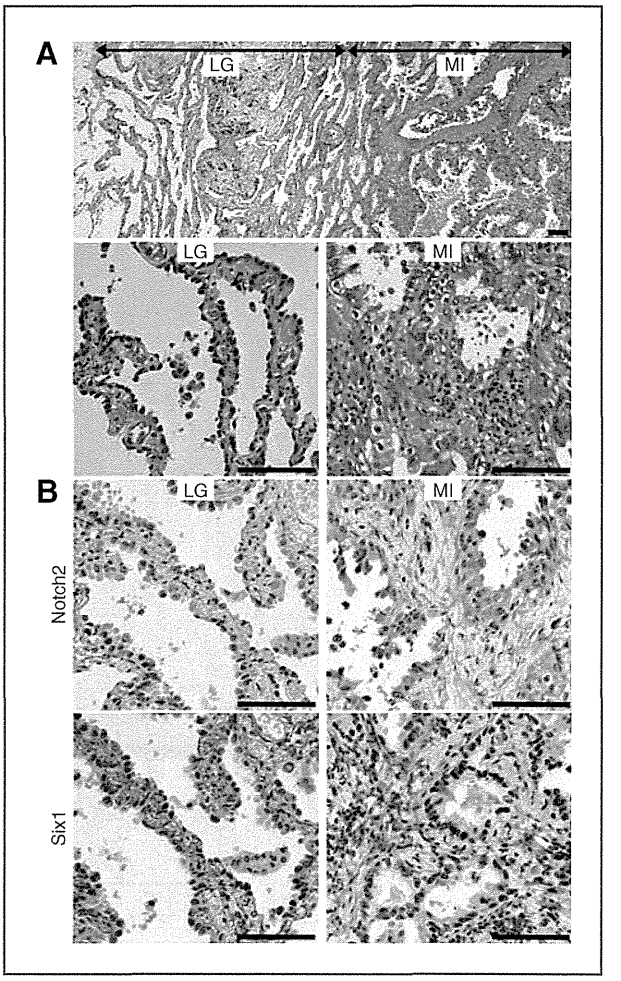


**Figure 3.** Immunohistochemical staining for Notch2 and Six1 on a minimally invasive adenocarcinoma. Serial sections of the minimally invasive adenocarcinoma from case 10 (listed in Fig. 2A and Supplementary Table S1) were stained with H&E (A) and immunostained with either the Notch2 or Six1 antibody (B). Representative staining images of the lepidic growth (LG) and microinvasion (MI) components are shown in the left and right panels, respectively. Bar, 100 μm.

morphology, NCI-H441 cells expressed easily and faintly detectable levels of *E-cadherin* and *vimentin*, respectively (Fig. 4A, lane 1). The expression levels of these two genes were inverse in NCI-H441 cells transfected with Notch2 ICD cDNA (Fig. 4A, lane 3 and Supplementary Fig. S2). Such transfection also resulted in *Smad3* and *Smad4* transactivation (Fig. 4A, lane 3 and Supplementary Fig. S2). Transfection with the empty vector did not alter the endogenous expression of these 4 genes (Fig. 4A, lane 2 and Supplementary Fig. S2). Transfection with TTF-1 resulted in *vimentin* transactivation and *E-cadherin* downregulation (Fig. 4A, lane 4 and Supplementary Fig. S2). Notch2 seemed to promote EMT in NCI-H441 cells more efficiently than TTF-1. NCI-H441 cells were transfected with Notch2 ICD cDNA and with either Six1-targeting siRNA or a control scrambled siRNA. The Six1-targeting siRNA abrogated not only Notch2 ICD–induced transactivation of *Six1* but also

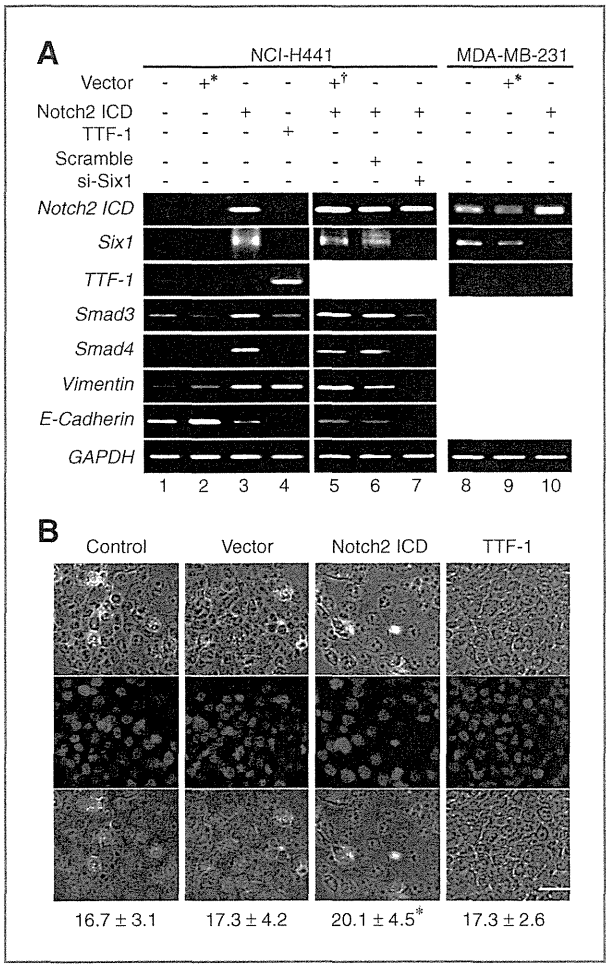


Figure 4. Transcriptional and cell morphologic alterations induced by exogenous Notch2 ICD in NCI-H441 cells. A, expression of EMT-related genes in NCI-H441 and MDA-MB-231 cells before and after transfection with various transcription factors and si-RNA. NCI-H441 and MDA-MB-231 cells were transiently transfected with pCX4-bsr empty (*lanes 2 and 9) or with vectors expressing either Notch2 ICD (lanes 3 and 10) or TTF-1 (lane 4). NCI-H441 cells were transiently transfected in some experiments with Notch2 ICD cDNA and with either empty pSilencer4.1-CMVneo (†lane 5) or vectors expressing scrambled (lane 6) or Six1-targeting (lane 7) siRNA. Total RNAs extracted from intact or transfected cells were analyzed by RT-PCR using primer set for indicated genes. Portions of PCR products were resolved by electrophoresis on 1% agarose gels. B, changes in sizes of nuclei in NCI-H441 cells transfected with Notch2 ICD cDNA. NCI-H441 cells were transfected or not (control) with either empty pCX4-bsr or vectors expressing cDNAs for Notch2 ICD or TTF-1 and then stained with DAPI to visualize nuclei (blue). Phase-contrast (top) and UV laser (middle) images of cells are merged (bottom). Sizes of nuclei were determined as described in Materials and Methods, and calculated means and SE are shown below the images. *, $P < 0.01$ compared with values of other types of cells. Bar, 50 μm.

that of *Smad3*, *Smad4*, and *vimentin*, whereas it further enhanced the Notch2 ICD–induced downregulation of *E-cadherin* (Fig. 4A, lane 7). Control transfection did not alter the gene expression induced by Notch2 ICD (Fig. 4A, lanes 5 and 6). These results indicated that Six1 is essential for Notch2 to transactivate *Smad3*, *Smad4*, and *vimentin*, but not to downregulate *E-cadherin*.

Notch2 ICD transfection experiments, followed by RT-PCR, were conducted on 2 other lung adenocarcinoma cell lines, A549 and RERF-LC-MS, both of which expressed endogenously undetectable levels of Notch2 and Six1 (Supplementary Fig. S3). Exogenous Notch2 ICD in these cells induced gene expression alterations resembling those in NCI-H441 cells, except that *Smad4* and *E-cadherin* were not upregulated in A549 and RERF-LC-MS, respectively (Supplementary Fig. S3). These results suggested that Notch2 and Six1 played pivotal roles in inducing EMT of lung adenocarcinoma cells.

Early-stage lung adenocarcinoma progression is assumed to be associated with an increase in the size of cancer cell nuclei (8). We measured the greatest dimension of cancer cell nuclei in 5 minimally invasive adenocarcinomas and found significantly larger nuclei in microinvasion, than in lepidic growth cancer cells from all 5 minimally invasive adenocarcinomas (Supplementary Table S1). A comparison between intact NCI-H441 cells and those transfected with the Notch2 ICD cDNA showed significantly larger nuclei in the transfectants than in the intact cells (Fig. 4B). Transfection with empty vector or with TTF-1 cDNA did not alter the size of nuclei in NCI-H441 cells (Fig. 4B).

### Upregulation of Notch2 and Six1 defines a clinically aggressive phenotype of lepidic-predominant invasive adenocarcinoma

We immunohistochemically analyzed 64 samples of lepidic-predominant invasive adenocarcinoma tumors using antibodies against Notch2 and Six1. Table 1 summarizes the clinicopathologic features of each case. The immunohistochemical staining results were judged positive when more than 50% of the cancer cells in each of the lepidic growth and overt invasion components had significant cytoplasmic (Notch2) or nuclear (Six1) staining. The tumors were classified based this judgment as double (Notch2 and Six1) negative in lepidic growth, but double positive in overt invasion (N/P; $n = 23$) cells; double negative in both components (N/N; $n = 19$); double positive in both components (P/P; $n = 19$) and other ($n = 3$; summarized in Table 1). A representative staining profile of N/P tumors was shown in Supplementary Fig. S4. A statistical analysis of the clinicopathologic parameters among the groups showed that the N/P group was less favorable than the N/N group with respect to pT, pN, PL factor, and ly factor (Table 1). Univariate log-rank analyses of Kaplan–Meier survival curves revealed that DFS duration was shorter in the N/P, than in the N/N group ($P = 0.015$; Fig. 5). DFS duration was also affected by various clinicopathologic parameters including pStage, pT, pN, PL factor, and ly factor (Supplementary Table S3). Multivariate logistic regression analyses among the 3 groups revealed that the N/P and P/P groups were more likely to recur than the N/N group in 2-year postoperative follow-up (Supplementary Table S4).

**Table 1.** Classification of patients with lepidic-predominant invasive adenocarcinoma according to Notch2 and Six1 immunohistochemical findings

| | | Notch2 and Six1 | | | | | |
|---|---|---|---|---|---|---|---|
| **Variable** | **All patients** | **N/N** | **N/P** | **P/P** | **Other** | | ***P*** |
| Sex | | | | | | N/N vs. N/P | 0.59 |
| Male | 36 | 10 | 14 | 11 | 1 | N/N vs. P/P | 0.74 |
| Female | 28 | 9 | 9 | 8 | 2 | N/P vs. P/P | 0.85 |
| Age | | | | | | N/N vs. N/P | 0.95 |
| Mean | 71 | 70.5 | 70.7 | 70.8 | 78.3 | N/N vs. P/P | 0.93 |
| Range | 49–86 | 49–86 | 58–83 | 56–85 | 74–85 | N/P vs. P/P | 0.97 |
| pStage[a] | | | | | | N/N vs. N/P | 0.33 |
| IA + IB | 52 | 17 | 18 | 14 | 3 | N/N vs. P/P | 0.21 |
| IIA + IIB + IIIA + IIIB | 12 | 2 | 5 | 5 | 0 | N/P vs. P/P | 0.73 |
| pT[a] | | | | | | N/N vs. N/P | 0.04 |
| 1a + 1b | 39 | 15 | 11 | 11 | 2 | N/N vs. P/P | 0.16 |
| 2a + 2b + 3 | 25 | 4 | 12 | 8 | 1 | N/P vs. P/P | 0.52 |
| pN[a] | | | | | | N/N vs. N/P | 0.03 |
| 0 | 55 | 19 | 18 | 15 | 3 | N/N vs. P/P | 0.03 |
| 1 + 2 | 9 | 0 | 5 | 4 | 0 | N/P vs. P/P | 0.96 |
| PL factor[a] | | | | | | N/N vs. N/P | 0.005 |
| 0 | 50 | 18 | 13 | 17 | 2 | N/N vs. P/P | 0.55 |
| ≥1 | 14 | 1 | 10 | 2 | 1 | N/P vs. P/P | 0.02 |
| ly Factor[a] | | | | | | N/N vs. N/P | 0.039 |
| 0 | 46 | 18 | 16 | 10 | 2 | N/N vs. P/P | 0.003 |
| 1 | 18 | 1 | 7 | 9 | 1 | N/P vs. P/P | 0.26 |
| v Factor[a] | | | | | | N/N vs. N/P | 0.67 |
| 0 | 56 | 18 | 21 | 14 | 3 | N/N vs. P/P | 0.08 |
| 1 | 8 | 1 | 2 | 5 | 0 | N/P vs. P/P | 0.13 |
| Tumor size (mm) | | | | | | N/N vs. N/P | 0.89 |
| Mean | 25.3 | 25.5 | 25 | 24.7 | 30 | N/N vs. P/P | 0.82 |
| Range | 11–70 | 11–70 | 15–40 | 12–38 | 15–50 | N/P vs. P/P | 0.87 |

[a]According to TNM classification (7th Edition).

## Discussion

This study comprised 3 parts. A clinical issue had to be considered for the first part that compared comprehensive gene expression between lepidic growth and microinvasion cancer cells in individual minimally invasive adenocarcinomas. Because the cut surface at the greatest dimension of the tumor is used for pathologic diagnosis, remaining specimens for LMD contained only a small amount of each component, particularly the microinvasion component. The original estimated amount of total RNA used for the present DNA microarray analysis was in the order of 100 ng per component or less. This limitation might have caused considerable RNA degradation and consequently resulting in shorter aRNA probes (theoretical average length, ~1.5 kb) (Fig. 1C). Regardless, the DNA microarray analysis seemed reliable because (i) the range of the relative expression levels of 10 housekeeping genes was sufficiently small

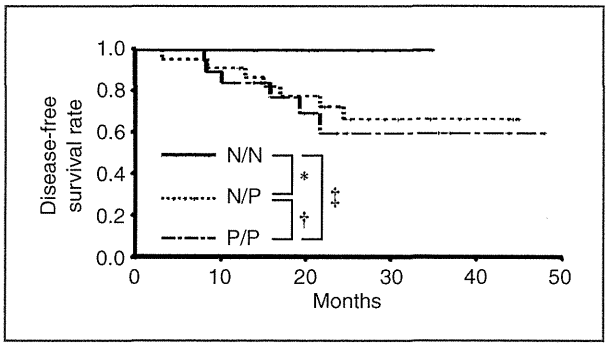


**Figure 5.** DFS rates of 64 lepidic-predominant invasive adenocarcinomas grouped by Notch2 and Six1 immunohistochemistry. DFS rates of N/N, N/P, and P/P tumor groups shown as function of months. The mean interval of DFS (95% CI) for N/P and P/P are 34.9 (28.8–41.1) months and 34.7 (26.2–43.2) months, respectively. Values for N/N were not calculated because N/N tumors did not recur. *, $P = 0.015$; †, $P = 0.626$; ‡, $P = 0.006$.

(within 0.5- to 2-fold) between lepidic growth and microinvasion cells (Supplementary Table S2), and (ii) differential expression of the selected 2 genes, that is, *Notch2* and *Six1* genes, was reproducibly confirmed by RT-PCR (Fig. 2A, case 1). These results indicate that tumor lesions at the early stage that contain cancer cells with different malignant potential, for example, *in situ* and invasive cells in minimally invasive adenocarcinoma, are practical for comparative gene expression analyses among cancer cells during progression *in vivo*.

Both *Notch2* and *Six1* were upregulated in microinvasion cancer cells not only in the minimally invasive adenocarcinoma that was analyzed using DNA microarrays but also in 10 other minimally invasive adenocarcinomas examined. We therefore considered that paired upregulation of Notch2 and Six1 is commonly associated with the progression of lepidic growth to microinvasion cancer cells in minimally invasive adenocarcinoma. Notch2 is a cell membrane–bound ligand-dependent receptor for the Type 1 transmembrane protein family named Notch (30–33). When Notch ligands bind to Notch2 receptors between two neighboring cells, Notch2 is cleaved through a cascade of proteolytic enzymes, including γ-secretase, and released Notch2 ICD translocates into the nucleus where it transcriptionally activates Notch2 target genes (26). Although Notch1 and Notch3, other members of the Notch family, have long been regarded as candidate molecules responsible for the development of lung cancer (34–36), whether Notch2 has similar roles remains to be determined. Six1 is a homeodomain transcription factor (37) and a putative downstream target of Notch2 (24, 25). Interestingly, Ford and colleagues showed that Six1 stimulates the malignant transformation of mammary epithelial cells through transactivating *cyclin A1* (38, 39) and induces EMT in mammary cancer cells through the induction of TGF-β signaling (27, 40). These findings suggested that Notch2 and Six1 play coordinate roles during the early-stage lung adenocarcinoma progression.

The second part of this study examined this notion using transfection experiments. Consistent with previous characterization, exogenous expression of the Notch2 ICD resulted in *Six1* transactivation in NCI-H441 lung epithelial cells. The exogenous Notch2 ICD also transactivated *Smad3*, *Smad4*, and *vimentin* in association with the downregulation of *E-cadherin*. Similar transactivation effects of Notch2 ICD were detected in 2 other types of epithelial cells derived from lung adenocarcinomas. Interestingly, Six1 was notably essential for transactivation of the 3 genes, but not for the downregulation of *E-cadherin*, suggesting that Notch2 and Six1 coordinately played a causative role in inducing EMT during the progression of lepidic growth to microinvasion cells. Exogenous expression of the Notch2 ICD in NCI-H441 cells also resulted in nuclei becoming enlarged. This was in accordance with the cytologic finding that nuclei were larger in microinvasion cancer cells than in lepidic growth cells from 5 minimally invasive adenocarcinomas examined. These results supported the notion that the transcriptional cascades activated coordinately by Notch2 and Six1 are involved in lepidic growth-to-microinvasion progression.

The third part of the study immunohistochemically investigated Notch2 and Six1 in 64 samples of lepidic-predominant invasive adenocarcinoma tumors and found that they could be assigned almost equally into groups on the basis of positive and negative staining as N/N, N/P, and P/P. Consistent with the results of the second part of the study showing that Six1 is a downstream target of Notch2, these transcription factors were either double negative or double positive in lepidic growth and overt invasion cancer cells, respectively, with some exceptions. As might be predicted from the diagnostic criteria, lepidic-predominant invasive adenocarcinoma seemed to include heterogeneous tumors with distinct natural histories and genetic alterations. Judging from the immunostaining profiles of lepidic growth and overt invasion cells, N/P tumors seem to be a simple advanced form of minimally invasive adenocarcinoma, in which microinvasion cells have grown into an overt invasion focus, and N/N tumors develop via other molecular mechanisms than those involving Notch2 and Six1. On the other hand, the origin of P/P tumors is uncertain, but they might be a more advanced form of N/P tumors. Because lepidic growth cancer cells were positive for both Notch2 and Six1, they might be potentially invasive. This speculation is reminiscent of a recent report by Anami and colleagues who notably pointed out that the lepidic growth pattern might represent the intraalveolar epithelial spread of overt invasion cancer cells (41). Whether or not lepidic growth cancer cells are invasive did not seem to affect the prognostic outcomes of patients with lepidic-predominant invasive adenocarcinomas (N/P vs. P/P in Fig. 5). Interestingly, we found that N/N tumors metastasized less often to lymph nodes, were less invasive to lymphatic vessels, and were associated with better DFS than N/P and P/P tumors ($P = 0.015$ and 0.006 by log-rank tests, respectively). These findings agree with a summary of reviews that emphasize the critical role of Notch signals in the malignant progression of non-small cell lung cancer (34–36). The paired upregulation of Notch2 and Six1 seemed to be one transcriptional alteration that is responsible for minimally invasive adenocarcinoma-to-lepidic-predominant invasive adenocarcinoma progression, and it defined a clinically aggressive phenotype subset of lepidic-predominant invasive adenocarcinoma. Because Notch2 and Six1 immunohistochemistry seemed to independently discriminate lepidic-predominant invasive adenocarcinomas with high risk of recurrence in a 2-year postoperative period, during which the recurrence of most lung cancers occurs even after curative-intent therapy (42), it could be a clinically useful examination for selecting patients with lepidic-predominant invasive adenocarcinoma needing intensive follow-up.

Aviel-Ronen and colleagues (2008) examined genomic changes associated with adenocarcinoma *in situ* and minimally invasive adenocarcinoma using array comparative